Performance of 54-Year-Old Prestressed Concrete Channel Beams with MF-FRP Repairs after 2 years of Restored Service

NCDOT Project 2024-15
FHWA/NC/2024-15
May 2026

NC STATE UNIVERSITY

Kendon Gann, Gregory Lucier,
Rudolf Seracino, Mohammad Qambar,
and Taylor Brodbeck

RESEARCH & DEVELOPMENT

Performance of 54-Year-Old Prestressed Concrete Channel Beams with MF-FRP Repairs after 2 Years of Restored Service

FINAL REPORT

Submitted to:
North Carolina Department of Transportation
Office of Research
(Research Project No. RP2024-15)

Submitted by:

Graduate Research Assistant: J. Kendon Gann, M.S.

Principal Investigator: Gregory W. Lucier, Ph.D.

Other Investigators:
Rudolf Seracino, Ph.D.
Mohammad Qambar, Ph.D.
Taylor Brodbeck, Ph.D.

North Carolina State University
Constructed Facilities Laboratory

2414 Campus Shore Dr., Raleigh, NC 27606
919-513-7322

gwlucier@ncsu.edu

May 31, 2026

Technical Report Documentation Page

1. Report No. FHWA/NC/2024-15	2. Government Accession No.	3. Recipient's Catalog No.
4. Title and Subtitle Performance of 54-Year-Old Prestressed Concrete Channel Beams with MF-FRP Repairs after 2 Years of Restored Service		5. Report Date May 31, 2026 6. Performing Organization Code
7. Authors J. Kendon Gann, Gregory Lucier, Rudolf Seracino, Mohammad Qambar, and Taylor Brodbeck		8. Performing Organization Report No.
9. Performing Organization Name and Address North Carolina State University Department of Civil, Construction, and Environmental Engineering Constructed Facilities Laboratory Raleigh, NC 27695-7908		10. Work Unit No. (TRAIS) 11. Contract or Grant No.
12. Sponsoring Agency Name and Address North Carolina Department of Transportation Research and Development Unit 1549 Mail Service Center Raleigh, North Carolina 276699-1549		13. Type of Report and Period Covered Final Report 08/01/2023 - 12/31/2025 14. Sponsoring Agency Code NCDOT Project RP2024-15
15. Supplementary Notes		

16. Abstract

A prestressed mechanically fastened fiber-reinforced polymer (MF-FRP) retrofit system was previously developed to provide a rapid, cost-effective means of extending the service life of deteriorated prestressed concrete bridges. Designed for short-term use and to be installed without specialized equipment, the system enables certain degraded bridges to remain open, often without load posting, until full permanent replacement projects can be planned, scheduled, and completed.

The static performance of the MF-FRP system was previously verified through laboratory tests of full-scale prestressed channel beams removed from structures approximately 54 years old. In these prior NCDOT research efforts, new MF-FRP components were installed in the laboratory on old beams. The prior research was followed by installations of the MF-FRP system on three in-service prestressed concrete C-channel bridges in North Carolina, each of which was about 54 years old at the time of retrofit and remained in service for approximately another two years while replacement projects were planned, scheduled, and implemented.

Demolition of two of these bridges during replacement presented the opportunity to salvage five retrofitted beams and seven companion control beams as part of the current research project. The current effort included full-scale static and fatigue tests of the salvaged girders to evaluate the condition and performance of the aged beams, some of which included field-applied retrofits subjected to about two years of environmental exposure and traffic loading. Results show that when the MF-FRP system is installed on both stems of a channel member, the capacity of that member is increased beyond the original design levels. Installations of MF-FRP on a single stem of a channel member are not recommended due to poor experimental performance. Fatigue tests designed to simulate up to an additional three years of field service demonstrated that strengthened members performed well in fatigue, with significant useful life remaining in the repaired members at the time they were removed from the field. All observed fatigue failures occurred in the concrete rather than in the mechanical components of the MF-FRP system, enabling inspection guidance to be proposed and indicating good durability of the MF-FRP system. Based on these findings, the recommended service life of the MF-FRP retrofit can be extended from two years to five years, provided retrofitted members are regularly inspected.

17. Keywords Prestressed concrete bridge beams; channel beams; cored slabs; FRP; mechanically-fastened repair; retrofit; fatigue; cyclic	18. Distribution Statement		
19. Security Classif. (of this report) unclassified	20. Security Classif. (of this page) unclassified	21. No. of Pages 60	22. Price

Form DOT F 1700.7 (8-72) **Reproduction of completed page authorized**

DISCLAIMER

The contents of this report reflect the views of the authors and not necessarily the views of North Carolina State University. The authors are responsible for the facts and the accuracy of the data presented herein. The contents also do not necessarily reflect the official views or policies of the North Carolina Department of Transportation at the time of publication. This report does not constitute a standard, specification, or regulation.

ACKNOWLEDGEMENTS

The authors would like to thank the North Carolina Department of Transportation (NCDOT) Research & Development Office and Structures Management Unit for sponsoring and supporting this research. Many dedicated NCDOT personnel extensively assisted the researchers throughout this project, in particular Nicholas Pierce, P.E., chair of the NCDOT Steering Committee. The authors are also grateful to the staff of the North Carolina State University (NCSU) Constructed Facilities Laboratory (CFL), especially Johnathan McEntire for his technical support and laboratory expertise. Assistance in the laboratory provided by undergraduate student William Dunn is also acknowledged and greatly appreciated. Finally, the research team would also like to thank S&C Construction, LLC and R.E. Burns & Sons Co., Inc. for their assistance in recovering girders for testing.

EXECUTIVE SUMMARY

A prestressed mechanically fastened fiber-reinforced polymer (MF-FRP) system was previously developed to retrofit certain deteriorated prestressed concrete bridge beams. The system was designed to be cost-effective, rapidly installed without special equipment, and easily inspected. The system was intended as a short-term retrofit to extend the service life of prestressed concrete bridges by increasing load postings or preventing closures, only until such time that replacement of the superstructure or bridge could be completed. The efficacy of the system was demonstrated in prior NCDOT research under laboratory conditions on full-scale prestressed channel beams and cored slabs taken from bridges that were in service for more than 40 years. As part of this prior work, three in-service prestressed concrete C-channel bridges in North Carolina were retrofitted with the MF-FRP system. These bridges each had their service life extended by two years while replacement structures were planned and completed. During demolition of Bridge No. 810003 in Sampson County and Bridge No. 910180 in Wake County, a total of five prestressed channel beams with MF-FRP retrofits were recovered and delivered to the North Carolina State University Constructed Facilities Laboratory for testing as part of the current research. Seven additional unstrengthened beams were also recovered from these structures to serve as control specimens both with and without laboratory-applied strengthening.

The primary goal of this research was to assess the condition of the 54-year-old beams with two-year-old retrofits after field service. The experimental program included full-scale destructive testing under static and cyclic conditions. Salvaging beams from actual structures provided the unique opportunity to test the condition of the aged beams and their field-applied retrofits after exposure to environmental aging and traffic for two years. The destructive testing portion of this research included multiple static and fatigue tests designed to assess the performance and remaining lifespan, if any, of the aged MF-FRP systems. For comparison, aged girders were strengthened in the laboratory with new MF-FRP and then fatigue tested. Testing new MF-FRP on aged girders provided a baseline assessment of repair performance under known loading without environmental effects, providing data otherwise not available from the beams repaired in the field.

The condition of the as-received beams was fully documented at the laboratory prior to testing and concrete cores were taken from all specimens. Static tests quantified the performance of the MF-FRP retrofit and showed that the field-installed retrofits, when applied to both stems, still enabled beam capacities above theoriginal design loads after two years of field service. Excellent performance was even observed from a specimen with heavy damage to the MF-FRP retrofit. In contrast, the configuration of MF-FRP applied to only one stem in a channel beam is not recommended, as field-strengthened specimens of this variety exhibited undesirable failure modes in the unstrengthened stem.

In fatigue, both the field-strengthened members (with underlying damage that necessitated strengthening in the first place) and comparable unstrengthened members (with no visual damage) all generally performed well under cyclic loading and unloading that simulated several years of heavy truck traffic. These results support recommendations that the service life of the MF-FRP retrofit should be extended to a maximum of five years (at the AADT level used in this research) provided regular inspections are taking place. Regular inspections are justified and should focus primarily on the underlying prestressed concrete member as all failures from cyclic loading observed in this research occurred in the concrete section and concrete anchorage areas, not in the mechanical components of the MF-FRP system. Lastly, this research supported repairs of two additional deteriorated prestressed channel beam bridge in North Carolina, with installation of one system complete and the second system underway.

TABLE OF CONTENTS

LIST OF FIGURES

LIST OF TABLES

1 Introduction

1.1 Background

Prestressed concrete (PC) elements are a common bridge superstructure system used by the North Carolina Department of Transportation (NCDOT) and across the United States. Prestressed C-channel beams and prestressed cored slabs are found on many smaller-to-medium size structures across North Carolina (NC), especially in the central and eastern regions of the state. After being in service for roughly fifty years, many of these bridge elements are degrading due to overloaded traffic and environmental conditions that cause concrete to deteriorate and prestressing strands to corrode. These common issues are shown in Figure 1-1 and can present safety and operating concerns to structure owners, especially state Departments of Transportation (DOTs). Prestressing strand corrosion is one of the most common factors responsible for bridge deterioration that necessitates reducing load capacity. If deterioration prevents the bridge from meeting the load limits or service-related limits imposed by the American Association of State Highway and Transportation Officials (AASHTO), DOTs are required to remedy the problem (AASHTO, 2018). These remedies usually take the form of bridge or superstructure replacements, often accompanied by load-posting or complete closure of the older bridge while the replacement is planned, scheduled, and constructed. Replacement of the bridge is often the most practical and effective long-term option; however, replacements require extensive planning, permitting, budgeting, and time to complete the work. Load-postings, or complete or partial closures, are commonly utilized in the interim since they are rapid solutions for keeping the bridge safe. Posting and closures are also low-cost in terms of materials and manpower spent to implement them, however, the opportunity costs of interrupted use can be significant. Of the 138 bridges that utilize C-channel beams in NC, 112 are currently load-posted, with none currently closed (NCDOT, 2025). In addition, there are 3,554 cored slab bridges in NC; among these, 14 are load-posted and 1 is closed (NCDOT, 2025). Reducing disruptions to the community caused these postings and closures would require an effective retrofit action that could be implemented reasonably quickly and at a reasonable cost. Reopening closed bridges and allowing other degraded bridges to remain open with no or limited load-postings during the time permanent replacements are implemented would help maintain functionality of the bridge network and would minimize the inconvenience and cost that detours or closures bring to the community.

Figure 1-1: Example of a deteriorated prestressed concrete C-channel bridge beam (Bridge No. 070018)

An effective retrofit system for channel beams and cored slabs must address two key engineering criteria. The first of these relates to the inventory rating level (IRL), defined by AASHTO as “a live load, which can safely utilize an existing structure for an indefinite period of time” (AASHTO, 2016). This research and NCDOT both define a zero-tension stress limit in the concrete to ensure conservative calculation of the IRL, regardless of the location of a bridge within NC. The second engineering criterion is the operating

rating level (ORL), which is defined by AASHTO as "load ratings that generally describe the maximum permissible live load to which the structure may be subjected" (AASHTO, 2016). While this loading may allow the structure to experience minor damage, this damage is considered infrequent and is predicted to accumulate slowly. For the retrofit to restore a deteriorated prestressed bridge under the inventory and operating rating levels, that retrofit must actively restore any lost prestressing. Passive retrofit options could strengthen the structure from the perspective of ultimate capacity but could not remedy the required zero-tensile stress state.

A retrofit solution was previously developed under prior NCDOT research that utilizes a prestressed mechanically fastened fiber-reinforced polymer (MF-FRP) system (McCoy, 2019). The retrofit was studied to assess the ability of the system to improve or eliminate load postings on channel beam and cored slab bridges, including keeping bridges open that were closed or candidates for closure. The system used in this research is composed of an FRP plate, steel connecting elements and hardware, and a steel turnbuckle system, as shown in Figure 1-2.

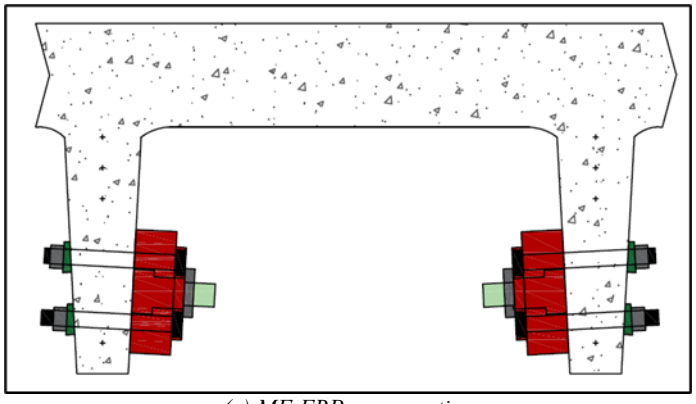

(a) MF-FRP cross section

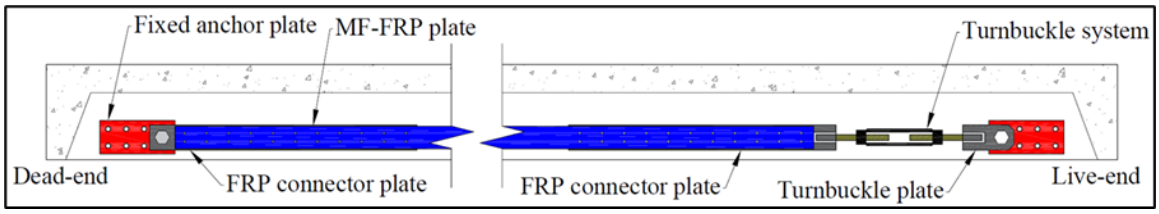

(b) MF-FRP schematic

Figure 1-2: Components of the MF-FRP retrofit solution from McCoy (2019)

While bridges are subject to cyclic loading, the experimental testing conducted in this earlier work on beams strengthened with the MF-FRP system included static loading only. This report on the current research outlines fatigue testing conducted on girders, including retrofitted girders in service for two years. The goal of the current work documented in this report is to quantify the effectiveness of the retrofit system after two years in service to better determine the useful lifespan of the repair.

1.2 Motivation and Research Significance

C-channel bridges are common structures to many state DOTs, and the deterioration of these structures is a common cause for concern. As explored in previous studies, load-postings and closures of these kinds of structures result in costly detours, increasing response time for emergency services, and disrupting local industries and agriculture. For these reasons, the MF-FRP retrofit system was developed and designed to extend the service life of prestressed concrete channel beams and cored slabs, minimizing disruptions to traffic.

The effectiveness of the retrofit system was previously proven, both with static and fatigue tests on the mechanical system components, and with static tests on channel beams strengthened with the retrofit system. Additionally, similar components were designed and tested on cored slab beams to allow for a wider range of applications. Successful field trials were implemented on several bridges, and MF-FRP system has now been in service long enough to see the replacement of bridges that previously had the retrofit installed. As a result, the opportunity to recover and test field-aged specimens strengthened with the system under static and fatigue loading configurations after two years in service was available at the start of the current research.

This research aims to provide additional data to expand the existing experimental database on the effectiveness of the system, and, more importantly, to quantify the useful lifespan of the system. Previous researchers have compiled data showcasing the effectiveness of the retrofit system and the ability of the system to address the flexural and shear deficiencies of candidate specimens (McCoy, 2019) (Bourara, 2019) (Lin, 2021). In addition, the methodology and design procedures used to implement the retrofit system have been developed and updated in a standard NCDOT design sheet. The performance of the system after being in service for two years needs to be evaluated through post-service laboratory fatigue testing because two years is the current recommended lifespan of the system. The critical question asked by this research is whether this recommendation is too short, just right, or too long.

1.3 Report Layout

The goal of this research is to add data points and to help fill knowledge gaps from previous studies, particularly as related to the fatigue performance of members strengthened with the MF-FRP system in-service. The tasks completed to achieve the goals of the research are included in the following eight Chapters:

- Chapter 2 contains a review of existing literature, including the previous studies conducted to develop and improve the system and study the fatigue performance of the mechanical components.
- Chapter 3 describes the full-scale experimental program undertaken to investigate the performance of the MF-FRP retrofit system after two years in service. The prestressed concrete channel beams used in this program were previously retrofitted by Lin and stayed in service for about 2 years after those retrofits (Lin, 2021).
- Chapter 4 presents the results of the full-scale experimental program and associated material tests. These results were used to more accurately document system performance and lifespan, allowing for a clearer understanding of the duration for which the retrofit system is an option for state DOTs.
- Chapter 5 exhibits the analysis performed with the results from Chapter 4. This analysis compares data gathered in this current work with those from previous experiments, further rounding out the database of experimental results. Analysis of the current experiments especially helps designers and engineers quantify the available capacity of the system over time, enabling selection of a reasonable service life for the repair.
- Chapter 6 provides a summary of the work performed and recommendations for future work. Another bridge that is under consideration for retrofit by the NCDOT is shown. Details of this bridge, with condition photos, are included to highlight a scenario where the system would be ideal.
- Chapter 7 presents the plan for implementation of this research by the NCDOT.
- Chapter 8 presents conclusions from this research.

2 Literature Review

This chapter presents a review of prior work conducted on MF-FRP systems, including the results and the knowledge gaps that remain to be addressed. A more extensive literature review related to the design, long-term behavior, and shear behavior of the MF-FRP retrofit system used in this research can be found elsewhere (McCoy, 2019) (Bourara, 2019) (Lin, 2021) (Gann, 2025).

2.1 Review of Previous MF-FRP Studies

The MF-FRP retrofit system aims to restore prestress losses and strength reduction in mild to moderately deteriorated prestressed concrete superstructures to extend their useful service life (McCoy, 2019). The MF-FRP system consists of fixed plates anchored to the concrete with bolts; pin connections to attach the FRP connector plate and turnbuckle connection plates to the fixed plates; and the FRP plate which is attached to the FRP connector plates, as shown in Figure 2-1. McCoy found that by utilizing a 22-bolt pattern with 0.5 inch diameter bolts, the average useful tensile capacity of the system was 46.4 kips.

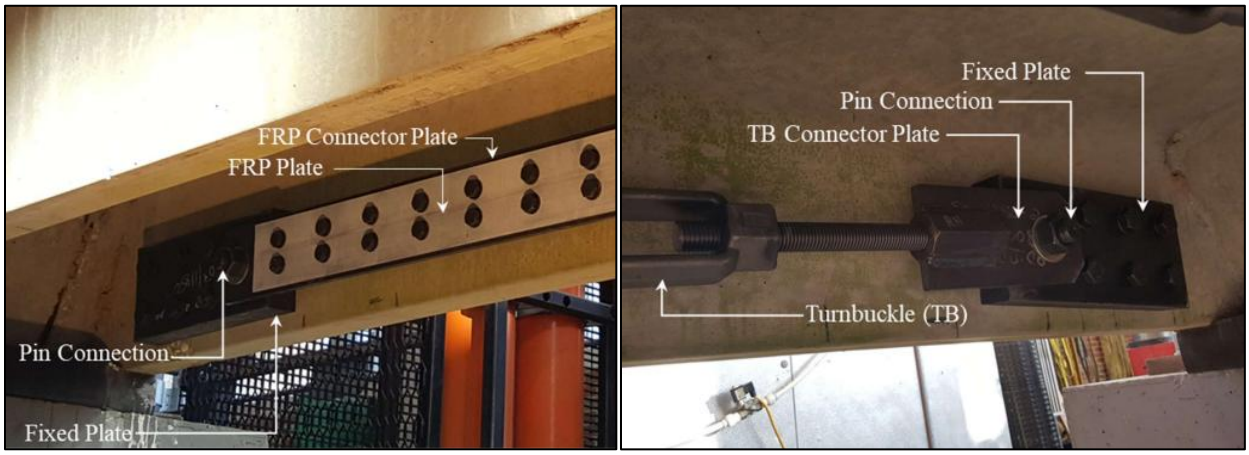

(a) Dead end *(b) Live end*

Figure 2-1: MF-FRP retrofit system components (adapted from (McCoy, 2019)).

Bourara studied the long-term behavior of the FRP-steel bolted connection under sustained and cyclic loads (Bourara, 2019). The effects of creep on the MF-FRP bolted connection were explored by subjecting two groups of specimens to different periods of sustained loading (6 months and 30 months). The specimens consisted of the 22-bolt pattern with 0.5-inch diameter bolts. It was found that the MF-FRP connection experienced creep within the first 5 days of sustained loading. This sustained load was 22 kips, which is the prestressing force of the system used in this study. A photo of the sustained loading test setup is shown in Figure 2-2. Under this sustained load, the connection experienced an average of 0.07 in. of creep, and the research concluded that the ultimate tensile capacity of the connection was unaffected by creep after 30 months of sustained loading.

Figure 2-2: Sustained loading test setup (adapted from (Bourara, 2019)).

The effects of cyclic loading on the MF-FRP bolted connection were explored by cycling the MF-FRP connection from 22 kips to 29 kips for a specific number of cycles; if the specimen did not fail in fatigue, the specimen was loaded to failure. This was completed through testing on a universal testing machine. The data from the cyclic loading tests was collected in the form of displacement measurements at each cycle. Bourara also conducted testing on 0.5-inch diameter bolts with varying levels of torque on the bolts. It was concluded that:

1. The behavior of the MF-FRP system under cyclic loading was highly sensitive to torque and bolt size.
2. Damage in the form of longitudinal shear cracks slowly formed and worsened with each cycle.
3. For 0.5-in. diameter bolts with an applied torque of 60 ft.-lbs., the failure envelope shown in Figure 2-3 was developed for the tests concluded.
4. Damage accumulated slowly and steadily up to nearly 300,000 cycles, where, at 0.24 in., the damage started to grow rapidly until failure.
5. The FRP plates should be inspected routinely on installed retrofits, and that if displacements exceeded 0.24 in. with for 0.5-inch diameter bolts, then the plates should be replaced at that time.

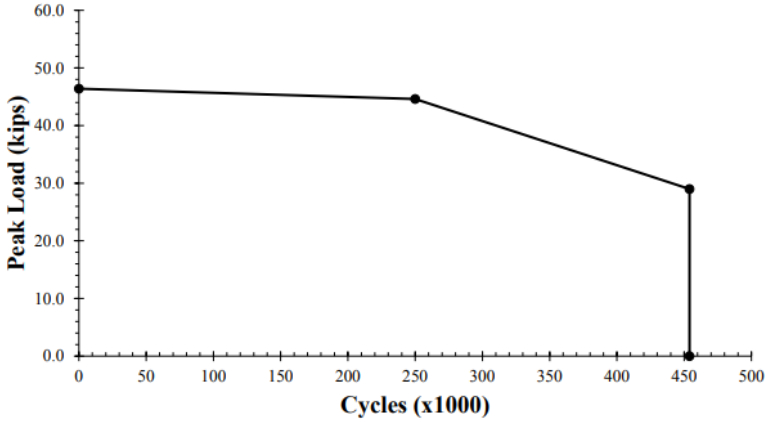

Figure 2-3: Failure envelope for 0.5-inch diameter bolts at 60ft.-lbs of torque (reproduced from (Bourara, 2019)).

Lin studied and developed a shear-strengthening plate for the end regions of candidate retrofit specimens (Lin, 2021). Through full-scale testing of channel beams in shear and flexure, Lin concluded that repairing specimens with the shear strengthening plate could restore the nominal shear capacity of a severely damaged beam end region to that of an undamaged beam. Implementation of the shear strengthening also caused the shear-deficient specimen to fail in flexure during a shear test, as shown in Figure 2-4. Concrete crushing under the loading apparatus defined this flexure failure.

(a) Dead end *(b) Live end*

Figure 2-4: Lin shear test failure mode (adapted from (Lin, 2021))

The aforementioned researchers all contributed full-scale tests to a database demonstrating how the MF-FRP retrofit specimens perform. The number of tests, specimen type and configuration, and results are summarized below to allow for comparison later in this report.

McCoy tested 6 prestressed channel beams in flexure. These specimens included undamaged and damaged control specimens with no MF-FRP, two undamaged MF-FRP retrofitted specimens, and two damaged MF-FRP retrofitted specimens. A drawing of the test setup used is shown in Figure 2-5 and the results from these tests are shown in Table 2-1. A detailed description of the relevant results is provided in Chapter 5.

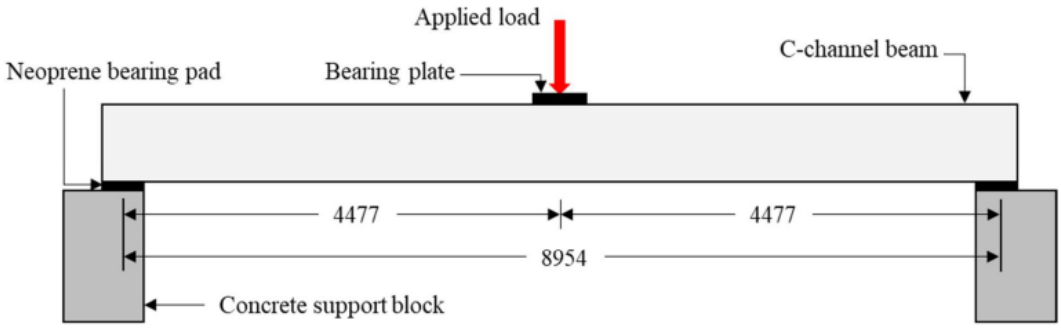

Note: All dimensions are in millimeters, 1 inch = 25.4 millimeters

Figure 2-5: Schematic of the McCoy test setup (reproduced from (McCoy, 2019))

Table 2-1: Results from the McCoy testing program (reproduced from (McCoy, 2019))

Specimen ID	U	D	MF-FRP-U1	MF-FRP-U2	MF-FRP-D1	MF-FRP-D2
HS-15 Live Load, kN (kips)	71.3 (16.0)	71.3 (16.0)	71.3 (16.0)	71.3 (16.0)	71.3 (16.0)	71.3 (16.0)
Ultimate Load, kN (kips)	132 (29.6)	83.6 (18.8)	156 (35.1)	166 (37.3)	123 (27.6)	116 (26.1)
Percent increase from U, %	--	-36.6	18.1	25.8	-6.85	-12.1
Percent capacity of HS-15, %	185	117	219	233	172	163
Maximum measured FRP tensile strain, $\mu\varepsilon$	--	--	7380	6425	7980	6712
Maximum FRP tensile force,[1] kN (kips)	--	--	148 (33.2)	128 (29.0)	160 (36.0)	135 (30.3)
Failure Mode [2]	CC	CC	LS/R, CC	CC	LS/R, CC	CC

Notes: 1) obtained from strain gauge and application of Hooke's Law; 2) LS is longitudinal splitting, R is rupture, CC is concrete crushing

Bourara tested five cored-slab beams in four-point bending. The specimens included in that research are shown in Table 2-2 with the corresponding results shown in Table 2-3.

Table 2-2: The Bourara specimens (reproduced from (Bourara, 2019))

Specimen ID	Description
U-U	Undamaged and unstrengthened control
D-U1	Damaged (two strands cut) and unstrengthened
D-S1	Damaged (two strands cut) and strengthened
D-U2	Damaged (four strands cut) and unstrengthened
D-S2	Damaged (four strands cut) and strengthened

Table 2-3: Results from the Bourara tests (reproduced from (Bourara, 2019))

Specimen ID	U-U	D-U1	D-S1	D-U2	D-S2
Ultimate load (kips)	82.3	74.9	85.5	61.9	77.9
Percent increase from U-U (%)	0	-9.0	+3.90	-24.8	-5.35
Maximum FRP axial strain (με)	-	-	7231	-	7444
Maximum FRP axial force[1] (kips)	-	-	32.6	-	33.6
Percent of FRP tensile capacity (%)	-	-	70.3	-	72.4
Failure Mode[2]	CC	CC	LS/R, CC	CC	CC
Operating load (kips)	44.0	44.0	44.0	44.0	44.0
Operating deflection (in.)	0.66	0.36	0.17	1.23	0.25
Change in operating deflection (in.)	0	-0.3	-0.49	+0.57	-0.41
Original inventory load (kips)	22.3	22.3	22.3	22.3	22.3
Original inventory deflection (in.)	-0.21	-0.17	-0.37	-0.06	-0.33
Change in inventory deflection (in.)	0	+0.04	-0.16	+0.15	-0.12

Notes: 1) calculated using Hooke's Law (E_{FRP} = 9020 ksi); 2) LS=longitudinal splitting, R=FRP rupture, CC=concrete crushing

Lin tested four C-channel beams in both shear and flexure. Due to the shear focus of that research, not all of the specimens tested by Lin are directly relevant to the current topic. The results from these tests are shown in Table 2-4. A detailed description of the relevant results is included in the Chapter 5 discussion.

Table 2-4: Results from the Lin testing program (reproduced from (Lin, 2021))

Test No.	Beam No.	Specimen ID	Max. Applied Load (kips)	Measured Disp. at Max. Load Location (in.)	Total Span (in.)	Shear Span (in)	Applied Shear Force at Shear Span (kips)	Failure Mode
1	1	C-U-S2	57.0	4.72	352	40	50.5	Flexure and Shear
2		C-DS-S1	45.4	2.71	268		38.7	Shear
3	2	C-U-S1	58.4	1.51	352		51.8	Shear
4		C-IDS-S1	57.4	0.90	280		49.2	Shear
5	3	S-DS-S1-F	37.3	0.52	352		33.0	Shear
6		S-DS-S1-FS	45.0	2.33	280		38.6	Flexure
7	4	S-DFS-F-FS	27.1	5.66	352	176	13.6	Flexure

2.2 Research Need

The long-term behavior of prestressed MF-FRP retrofit systems in service when subjected to fatigue testing has, to the knowledge of the authors of this report, not been explored in previous literature. Waiting for retrofitted specimens to accumulate extensive use in service takes time. Therefore, the opportunity to investigate the behavior of in-service specimens provides valuable data. In addition, these data will provide a more confident understanding of and recommendation for the lifespan of the temporary MF-FRP retrofit system, factoring in the effects of environmental aging and live traffic in the field.

3 Experimental Program

The purpose of this full-scale experimental program is to study the long-term MF-FRP retrofit system behavior on in-service channel beams at the end of the current recommendation for system lifespan (2 years). Recent replacements of bridges in North Carolina that had MF-FRP retrofits installed provided the unique opportunity to conduct this research. The experimental program consists of static control testing, fatigue testing, and material testing. This chapter presents the conditions of each specimen prior to testing, the test setup, and the instrumentation used in this program.

3.1 Specimen Retrieval

A total of twelve 30-ft. long C-channel beams were obtained for this testing program, with eight coming from Bridge No. 810003 in Sampson County, NC, and four coming from Bridge No. 910180 in Wake County, NC. The eight prestressed concrete channel beams retrieved from Bridge No. 810003, the same bridge retrofitted by (Lin, 2021), consisted of three retrofitted beams and five unstrengthened beams. These beams were removed from the bridge location and hauled to a local contractor's yard in early 2023. Upon visual inspection, the condition of the beams varied, with concrete spalling present at the midspan and supports, prestressing strand corrosion present in multiple locations, and some damage observed to the existing MF-FRP retrofit system on one of the stems. However, the overall condition of the beams was fair. The beams were shipped to the Constructed Facilities Laboratory (CFL) in two loads (November 20th, 2023, and May 9th, 2024). Figure 3-1 shows the beams as they were stored in the contractor's yard and the delivery by truck to the CFL.

(a) Beams in contractors' yard

(b) Loading of beams onto truck

Figure 3-1: Bridge No. 810003 beams

The four C-channel beams retrieved from Bridge No. 910180 consisted of two retrofitted beams and two control beams. These beams were removed from the bridge location and hauled directly to the CFL on May

9th, 2024. Upon visual inspection, the condition of these beams was similar to those retrieved from Bridge No. 810003. Figure 3-2 shows the beams on Bridge No. 910180 prior to their removal, as well as their delivery by truck to the CFL.

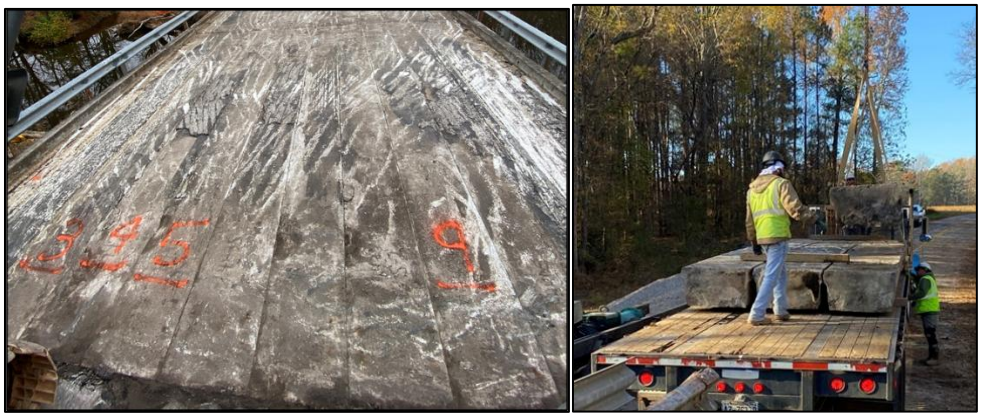

(a) Beams prior to removal *(b) Loading of beams onto truck*

Figure 3-2: Bridge No. 910180 beams

3.1.1 Specimen ID Nomenclature

After all beams were removed from their respective locations and trucked to the CFL, an ID was assigned to each specimen to distinguish them. The format used is as described: specimens are first labeled with "SC" or "WC" to denote the county of the donor bridge (Sampson County Bridge No. 810003 or Wake County Bridge No. 910180). A "U" is next in the ID if the beam is unstrengthened, while an "S" indicates that the specimen has the retrofit installed on both stems. In the cases where the specimen only had the retrofit on one stem, the "S" notation is modified by a footnote mentioning this specifically. The final integer distinguishes between the different strengthened and unstrengthened beams recovered from each bridge. For example, specimen SCU2 indicates a beam recovered from the Sampson County bridge that does not have the retrofit system installed and is the second beam of this configuration recovered from the bridge.

Table 3-1: Specimen IDs

Specimen ID	Bridge recovered from	Retrofit present?
SCU1	Sampson County	No
SCU2	Sampson County	No
WCU1	Wake County	No
SCS1	Sampson County	Yes
SCS2	Sampson County	Yes
WCS1*	Wake County	Yes*
WCS2*	Wake County	Yes*
SCS3	Sampson County	Yes
SCU3	Sampson County	No
WCS3	Wake County	Yes
SCU4	Sampson County	No
SCS4**	Sampson County	Yes**

*Retrofit installed on only one stem
**Retrofit applied in the laboratory using new MF-FRP

3.2 Prestressed Channel Beam Background Information

NCDOT specifications allowed for a suite of standard prestressed concrete channels that were approved and used consistently from the 1950s until cored-slab bridges became the norm many decades later. The interior channel beams from Bridge No. 810003 that are featured in this research had a specified minimum specified compressive strength at 28 days of f'_c = 5,000 psi, and a minimum required compressive strength at prestress transfer of 4,000 psi (North Carolina DOT, 1966). The prestressing strands used were 7/16" in diameter with an ultimate prestress force of 31 kips per strand. The NCDOT allowed three standard prestressing layouts, shown in Figure 3-3. The prestressing layout utilized by the specimens in this research program is Type A. Shown in Figure 3-3, each stem has four prestressing strands: one located on the bottom and three harped strands higher in the stem. The three harped strands are spaced at 7/16 in. on center at the point of depression, with the lowest harped strand located 6 in. up from the bottom of the stem at midspan. At the ends, these harped strands are spaced at 1.5 in. on center, with the lowest harped strand located 8.5 in. from the bottom of the stem. In addition to the prestressing strands, there are four No. 3 passive steel bars placed 2 in. from the top of the flange in the longitudinal direction.

The interior channel beams from Bridge No. 910180 are assumed to have the same reinforcement. This assumption was validated when plans from Bridge No. 810003 helped avoid hitting internal reinforcing steel during the drilling of core samples. The specified minimum compressive concrete strength of these beams is unknown.

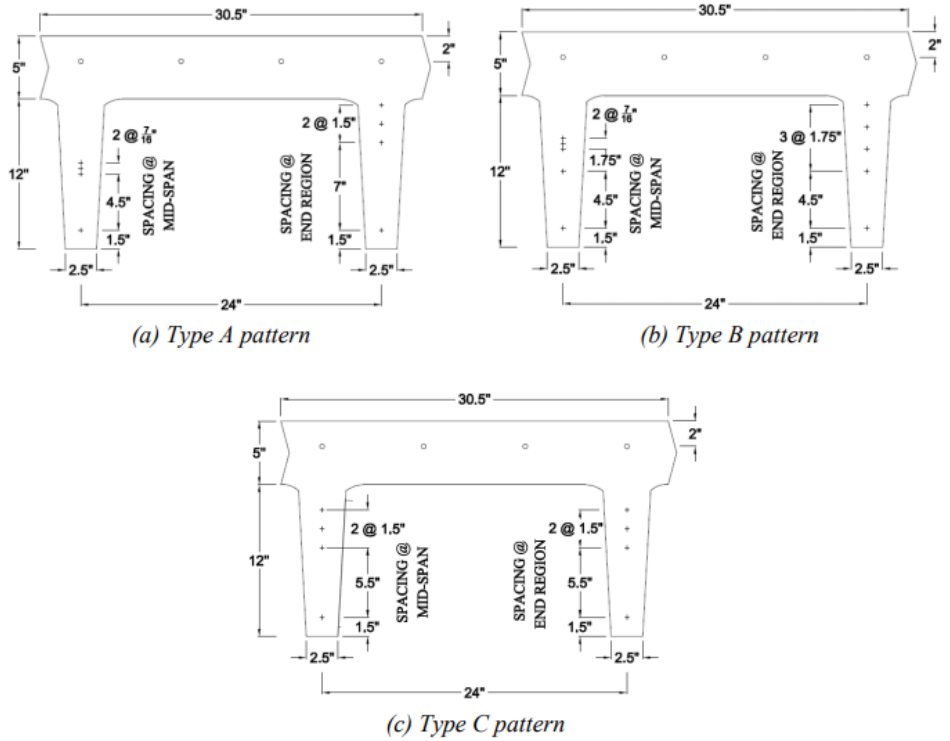

Figure 3-3: Standard C-channel beam cross-sections (adapted from (North Carolina DOT, 1966))

3.3 Loading Information

The interior C-channel beams from Bridge No. 810003 were designed with an original operating rating of HS-15 (North Carolina DOT, 1966). This corresponds to a 6-kip load on the steering axle and a 24-kip load on the tandem axles, seen in Figure 3-4. The 24-kip load on the tandem is split between both dual-wheel bearing areas. This means a single dual-wheel bearing area has a 12-kip load associated with it.

Due to the speed of a typical truck crossing the bridge, the use of an impact factor was justified; a truck traveling at a speed of 66 ft./s (45 miles per hour) would cross the bridge completely in less than half a second. Therefore, an impact factor of 1.33 (based on previous research by (McCoy, 2019)) is considered as this traffic load is considered dynamic. As such, the design load on an individual beam used to represent the original operating limit was 16 kips (an individual beam is wide enough to only support one dual-wheel load at a time when oriented parallel to the direction of travel).

In the "truck with trailer" case of HS-15 loading, the minimum spacing required between non-steering axles is 14 ft. Considering a beam span of 30 ft., the effect of one tandem was taken to model the design truck as any additional axles would have just entered or exited the bridge beam while the previous tandem was at midspan. As a result, three-point bending was selected for this research to accurately model the HS-15 design truck with the 30 ft. beam span.

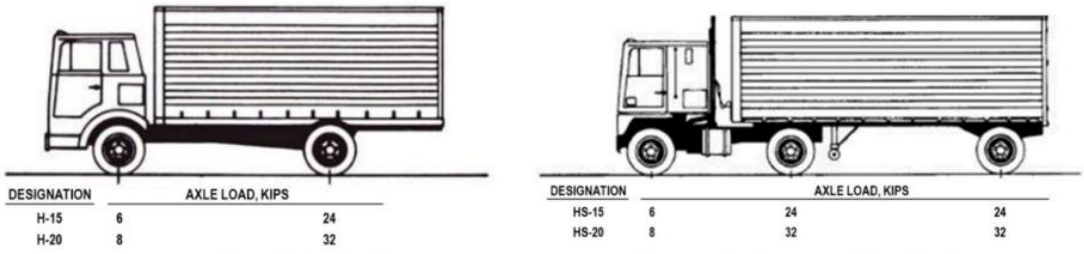

(a) single truck (H) loading *(b) truck with trailer (HS) loading*

Figure 3-4: AASHTO H/HS-15/20 design trucks (adapted from (AASHTO, 2016))

3.4 Testing Program

The MF-FRP retrofit system was installed by NCDOT on the bridges studied in this research to increase the capacity of selected beams back to their original operating load. These retrofits were necessary due to strand corrosion and associated loss of prestress force. The beams were about 54 years old at the time the retrofits were installed, and the bridges with the retrofits remained in service for another two years after retrofit installation.

When the retrofit bridges were scheduled for replacement in 2023, the decision was made to salvage several selected channel beams for laboratory testing, particularly channel beams with the aged MF-FRP retrofit installed. A testing program, outlined in Table 3-2 was created to assess the capacity of the aged beams, as removed from the field. In addition to static tests, the testing program also includes fatigue tests to assess the remaining service life of the aged strengthened beams at the time of their replacement.

Table 3-2: Test matrix table

Specimen	Strengthened/Unstrengthened	Test Type
SCU1	Unstrengthened	Static
SCU2	Unstrengthened	
SCU1	Unstrengthened	
SCS1	Strengthened	
SCS2	Strengthened	
WCS1*	Strengthened*	
WCS2*	Strengthened*	
SCS3	Strengthened	Fatigue
SCU3	Unstrengthened	
WCS3	Strengthened	
SCU4	Unstrengthened	
SCS4**	Strengthened**	

*Retrofit installed on only one stem

**Retrofit applied in the laboratory using new MF-FRP

3.4.1 Static Test Setup and Instrumentation

The static and fatigue testing programs were conducted in the Large Structural Systems Laboratory at the CFL. In the static testing program, beams were tested in a pin-roller configuration on a simple span. This was achieved by utilizing steel bearing plates grouted to the beam end-regions, which in turn rested on steel round stock. The round stock at one end of the beam was prevented from rolling to create a pin and was free to translate as a roller at the other end of the beam.

For consistency with the test setup previously utilized by McCoy, the members were tested in three-point bending (McCoy, 2019). A loading schematic is shown in Figure 3-5 showing a steel HSS tube loading element at midspan connected to two double-acting cylinders by two threaded rods with nuts and plates. The tube applied the load evenly to a 20 in. x 10 in. bearing plate on the top surface of the beam, in accordance with AASHTO bearing area requirements for wheel loading (AASHTO, 2017). A fiberboard intermediate layer was used to transfer a uniform pressure from the bearing plate to the concrete surface of the specimen. A photo of the loading apparatus is shown in Figure 3-6. To record the applied load, two load cells were utilized to measure the individual load from each cylinder. The two values were added together and recorded to provide the total applied load. Deflection during loading was also recorded by string potentiometers placed at the midspan of each stem. The deflection measured for each stem was used to calculate the average vertical midspan deflection of each beam.

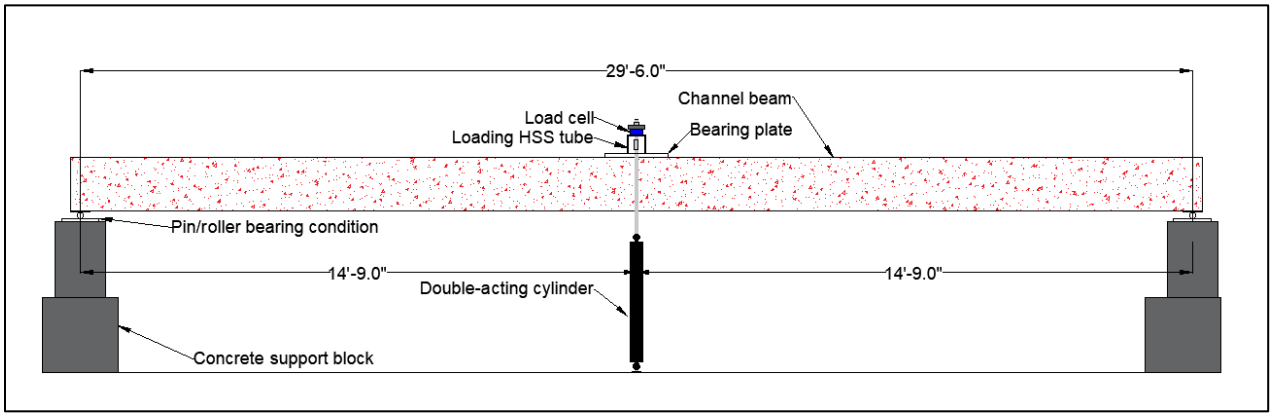

Figure 3-5: Static test setup schematic

Figure 3-6: Static test loading apparatus

Digital Image Correlation (DIC) was also implemented to measure the strain profile at the steel connector plate-FRP plate interface. For each test, both interfaces of one FRP plate were speckled and monitored during testing. DIC data was used to assess the behavior of the steel connector plate-FRP plate at failure. Figure 3-7 shows the speckling on one interface. The axial strain in the FRP plate was also measured using electrical resistance strain gauges. Three gauges, located at the top, middle, and bottom of each FRP plate, were utilized. Figure 3-8 shows the strain gauges on the FRP plate.

Figure 3-7: DIC speckling pattern

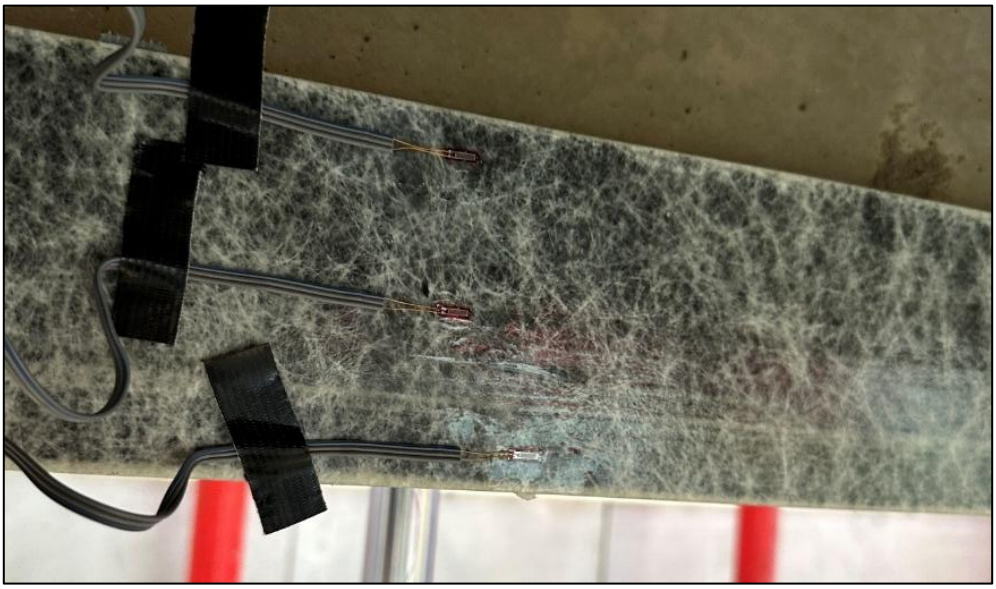

Figure 3-8: Strain gauges on FRP plate

The beams were tested under load-control conditions. The specimens were loaded to 8 kips, held under load for one minute, then unloaded. After this initial proof load, each beam was reloaded in 8-kip intervals until failure, stopping at points of interest such as major crack formation and propagation and prestressing strand rupture. A 16-kip point load corresponds to an internal midspan moment of 120 kip-ft, which is the live load moment generated by the original HS-15 vehicle loading condition, including impact, along a single wheel line for a 30-ft. span length (North Carolina DOT, 1966) (AASHTO, 2018).

3.4.2 Static Test Descriptions

A description of the condition of each static test specimen is presented in Table 3-3. A more detailed description of the condition of the test specimens, including photos, may be found elsewhere (Gann, 2025).

Table 3-3: Condition of static test specimens prior to testing

Specimen	Strengthening	Condition
SCU1	Unstrengthened	Concrete spalling near midspan on one stem, substantial concrete loss at one support.
SCU2	Unstrengthened	Concrete spalling along both stems and at end support; Some exposed mild reinforcement; bottom strand exposed on right stem, leading to section loss.
WCU1	Unstrengthened	Some concrete spalling at support.
SCS1	Strengthened w/ MF-FRP and shear strengthening plate	Concrete loss at support; significant spalling along one stem where bottom strand is almost completely exposed and corroded.
SCS2	Strengthened w/ MF-FRP	Significant corrosion led to bottom strand rupture on one stem; minor spalling on other stem. FRP plate heavily damaged on one stem, likely during demolition, with approximately 39% section loss of plate.
WCS1	Strengthened w/ MF-FRP, only one stem	Significant spalling on one stem, leading to bottom strand corrosion and rupture.

3.4.3 Fatigue Setup, Instrumentation, and Protocol

The fatigue tests used a setup similar to that described in the static testing program. The specimens were tested in a pin/roller configuration, achieved through the same methods mentioned previously. However, due to the long duration of fatigue tests, wider concrete supports were designed and cast to allow for cycling two specimens in parallel.

As was done in the static testing program, three-point bending was selected to deliver the load. To simplify the loading apparatus, a hole was drilled through the flange of the beams. This allowed a threaded rod to pass through and couple to a clevis, which was connected to a double-acting hydraulic cylinder. This cylinder was anchored through the strong floor. The threaded rod through the beam had a nut and a washer plate, which allowed the rod to pull down on a load cell, which was used to monitor the applied load. The load cell rested on a steel plate, which distributed the load to a 2 in. square HSS tube. This, in turn, distributed the load to the 10 in. by 20 in., 1 in. thick steel bearing plate, which applied the load to the specimen in accordance with AASHTO bearing area requirements for wheel loading (AASHTO, 2018).

Deflection was monitored using string potentiometers. However, due to the nature of fatigue, the string potentiometers were attached to the member for short, predetermined intervals during testing to avoid fatiguing the sensors themselves. To achieve this connection, a magnet was attached to the end of the wire coming from the beam stems, while a metal nut was attached to the wire coming from the string potentiometer. The metal nut could be coupled with the magnet as needed, allowing for the quick connection and disconnection of the string potentiometers from the cycling beam for data collection.

As previously mentioned, the supports allowed for two fatigue specimens to be independently run in parallel. Figure 3-9 shows a plan view of the fatigue test setup. The concrete support blocks were grouted on the bottom to allow for an even bearing on the strong floor. In addition, two concrete catch blocks were cast along with the supports. This ensured that the specimens could run continuously throughout the day without any worry of the surrounding laboratory settings being damaged if a member failed. A photo of the fatigue setup is shown in Figure 3-10.

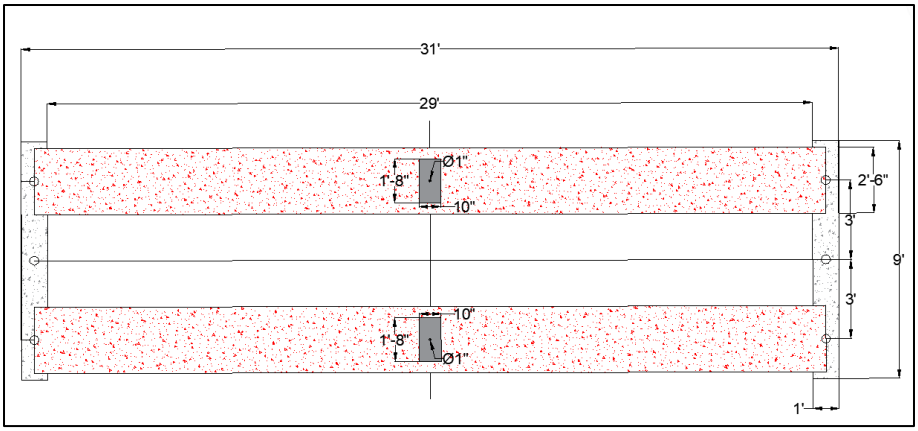

Figure 3-9: Plan view of fatigue setup

Figure 3-10: Fatigue test setup photo

Determining a fatigue load that allowed the system to be assessed in the most efficient way was of top priority. It was decided that assessing the performance of the system when fatigued at the operating load rating for this bridge was the best option; recall, the operating load is the maximum permissible live load the member should be exposed to, and incremental damage is expected to occur at this level. Although this loading is considered non-routine due to infrequent traffic, the member could potentially experience this level of load enough times over a long service life to warrant concern. Therefore, the operating load rating corresponding to a 16-kip point load was chosen for the upper bound of the fatigue load. The lower bound was taken to be 0 kips to simulate traffic moving off the bridge entirely.

Next, the number of cycles was determined to allow for a reasonable and conservative representation of the traffic that a generic bridge in rural North Carolina would see on a routine basis. Correlation was accomplished using traffic data from NCDOT traffic volume maps, and the average annual daily traffic (AADT) was found for both bridges studied in this research (NCDOT, 2024). However, this data alone did not directly provide the number of trucks included in the AADT (i.e. the heaviest loads that would be at or near the operating limit.) Therefore, an NCDOT traffic view tool was utilized to determine the percentage of commercial vehicles that make up the total traffic count (NCDOT, 2024). This value gave a more precise estimate of the number of trucks that the bridges might see in a typical year. The bus or commercial (BC) vehicle percentage of Bridge No. 810003 and Bridge No. 910180 were not available on direct routes crossing the bridges of interest, so data from surrounding roads that did have BC percentages available were used to estimate a BC percentage for each bridge. This data was tabulated, as shown in Table 3-4, and used to calculate a realistic and conservative number of cycles for the fatigue test.

The BC percentage varies by location across the state of North Carolina. To capture a value that is well-suited to represent many bridges across the state, a BC percentage of ten was selected. It should be noted

that the BC percentage includes all buses and smaller commercial vehicles, most of which likely do not produce the maximum assumed 16-kip point load on the member. Therefore, the 10% BC rate selected for use in this research is likely a very conservative estimate, thus creating a fatigue testing program that is likely more severe than actual field service.

Table 3-4: BC percentage of AADT

Bridge No.	AADT [Daily Axle Count]	Average Surrounding BC [%]	BC of AADT [Daily Axle Count]
810003	1100	12.4	136
910180	1900	6.4	122

After selecting a representative BC percentage, the number of high load cycles expected over a given period was calculated to determine the number of laboratory fatigue cycles necessary to represent an additional 3 years of service in the laboratory (Table 3-5). The number of axles near the operating load limit that will cross the bridge over three years of traffic (beyond the two years the members were already in service for) was conservatively estimated at just under 241,000. If those cycles simulating three additional years of service could be sustained, then beams with MF-FRP retrofits with two years of real service would be exposed to approximately 5 years of total service, the maximum duration of time potentially of interest to the researchers or to NCDOT for the temporary MF-FRP repair.

Table 3-5: Fatigue cycle calculation

AADT	1100	*vehicles*
Traffic cycles per year	**401500**	*vehicles*
No. of years for fatigue	3	*years*
Total cycles for fatigue	**1204500**	*vehicles*
Considering 10% BC loading		
No. of cycles due to trucks	**120450**	*trucks*
Tractor-Trailer (HS-15/20)	**240900**	*axles*

With the applied load and number of cycles defined, beams scheduled for fatigue testing were subjected to an initial static proof test to quantify the existing condition of each retrofitted beam. Condition was judged by the slope of the load-deflection data measured at midspan between applied loads of zero and 16 kips. As was done in the initial steps of the static test protocol, the static proof test loaded a specimen to 8 kips at a steady rate and held the applied load for one minute. The load was then released to zero before reloading the specimen to 16 kips. The deflection was measured at midspan and plotted versus the applied load. This result was used to quantify the stiffness of the specimen at the start of the fatigue cycles, and by comparing it to static test results of other specimens, to verify that it had sufficient capacity to undergo fatigue testing. Following a successful proof test, the beam was loaded in fatigue for up to 250,000 cycles. Beams successfully completing these cycles were then tested to failure using the static testing procedure previously outlined.

3.4.4 Fatigue Test Descriptions

This section describes the as-received condition of the six specimens tested in this report for fatigue following static proof tests. The condition is summarized in Table 3-6. All of the members appeared to be in acceptable condition other than Specimen WCS2, which had heavy concrete spalling and was only strengthened on one stem.

Table 3-6: Condition of fatigue test specimens prior to testing

Specimen	Strengthening	Condition prior to loading
WCS2	Strengthened w/ MF-FRP plate on one stem only	Stem with strengthening had substantial concrete spalling with the bottom strand completely corroded at midspan; top three strands also heavily corroded. Unstrengthened stem also exhibited heavy spalling and bottom prestressing strand was visibly corroded.
WCS3	Strengthened w/ MF-FRP plate	Concrete spalling was observed at locations where the shear reinforcement had corroded. A longitudinal splitting crack along the bottom of the right stem along the plane of the strengthening was observed at the back end of the beam, along with cracks around the bolt locations.
SCU3	Unstrengthened	Right stem had some spalling where shear reinforcement had corroded. A longitudinal splitting crack was observed at the front end of the beam on the left stem, as well as a hairline crack at midspan. Some patching was observed in the back end of the left stem. Concrete spalling was observed at midspan on the left stem; some wires of the bottommost prestressing strand appeared to have corroded.
SCU4	Unstrengthened	Some concrete spalling at the back end bearing location on the right stem. Minor concrete spalling at locations where shear reinforcement had corroded.
SCS3	Strengthened w/ MF-FRP plate	Minor concrete spalling along length of both stems, notably at the center. Bottom internal prestressing strand exhibited some corrosion but appeared intact and taut. The steel components of the MF-FRP system appeared rusty but in good condition with no visible damage. The FRP plate exhibited cracks along the bolt rows at the steel interface in the lab left front and lab left back directions. The other interfaces exhibited no visible damage.
SCS4	Strengthened w/ MF-FRP plate in the lab	Minor concrete spalling at bolt locations at front right end. Minor concrete spalling at locations where shear reinforcement had corroded. Concrete spalling along bottom of the stem at various locations on the right stem, exposing corroded prestressing strand. Note that this member appeared to be in good condition in the field, and so was only strengthened in the lab after being in-service.

3.5 Material Testing

To fully characterize and assess the performance of the specimens during testing, the concrete compressive strength of each specimen was determined by drilling concrete cores from each beam. Due to the varying location of the specified internal steel reinforcement and the available thickness of concrete, the core diameter of each core was limited to 2 in. Cores were extracted from each specimen after testing on that specimen concluded, with a goal of three cores per specimen. The ends of each core were cut with a wet tile saw to provide flat surfaces prior to grinding the bearing ends flat, smooth, and parallel in a specialized core grinder. The cores were then tested according to the relevant ASTM standards (ASTM C39-24, 2024) and (ASTM C42-20, 2020). Figure 3-11 shows a typical core in the testing machine. Using the recorded data, the concrete strength was calculated in accordance with ACI 214.4R (2010) (ACI 214.4R, 2010).

Figure 3-11: Typical concrete core in the compression testing machine

A total of 34 cores taken from the beams were tested in compression, and their peak loads were recorded. Table 3-7 summarizes the peak loads, standard ASTM factors applied to correct the compressive strength, and finally, the adjusted compressive strength of each core. Note that for all specimens, the correction factor f_{dia} was taken as 1.06 (correction for core diameter), f_{mc} as 0.96 (correction for moisture content), and f_d as 1.06 (correction for damage during coring); the correction for length-to-diameter ratio, $f_{l/d}$, for each core is tabulated below based on the individual dimensions. The design concrete strength for the bridge beams was 5.0 ksi. Only specimens SCU3 and WCU1 fell short of the design concrete strength by more than 300 psi; however, the relatively high variability in the strength of the extracted concrete cores is notable. The cores failed in the "Type 3" failure pattern defined in (ASTM C39-24, 2024). Peak loads for cores WCU1-1 and SCU3-3 were accidentally not recorded, so those tests are eliminated from the data set.

Table 3-7: Concrete core compression test results

Beam ID	Core ID	$f_{core,peak}$, psi	$f_{l/d}$	Adjusted f_{core}, psi	Average f_{core}, psi
SCU1	SCU1-1	7300	1.000	7871	7844
	SCU1-2	7787	0.997	8377	
	SCU1-3	6766	0.998	7285	
SCU2	SCU2-1	7281	1.000	7854	7500
	SCU2-2	7375	1.000	7952	
	SCU2-3	6297	0.985	6693	
SCU3	SCU3-1	3046	0.997	3275	3770
	SCU3-2	3954	1.000	4264	
SCU4	SCU4-1	5361	1.000	5782	6934
	SCU4-2	6931	1.000	7476	
	SCU4-3	6993	1.000	7543	
SCS1	SCS1-1	7862	0.999	8473	7683
	SCS1-2	6063	0.998	6528	
	SCS1-3	7469	0.999	8049	
SCS2	SCS2-1	5782	1.000	6236	6948
	SCS2-2	6878	0.999	7412	
	SCS2-3	6672	1.000	7194	
SCS3	SCS3-1	7309	0.999	7877	7339
	SCS3-2	6550	1.000	7065	
	SCS3-3	6560	1.000	7076	
SCS4	SCS4-1	6973	1.000	7522	7293
	SCS4-2	8210	1.000	8856	
	SCS4-3	5102	1.000	5502	
WCU1	WCU1-2	3889	0.999	4190	4305
	WCU1-3	4123	0.994	4420	
WCS1	WCS1-1	4348	1.000	4690	4860
	WCS1-2	5229	0.999	5635	
	WCS1-3	3945	1.000	4254	
WCS2	WCS2-1	4554	0.996	4891	4734
	WCS2-2	2970	0.974	3121	
	WCS2-3	5754	0.997	6188	
WCS3	WCS3-1	5454	1.000	5882	5437
	WCS3-2	5182	1.000	5590	
	WCS3-3	4489	1.000	4840	

4 Experimental Results

This chapter presents the experimental results of six static tests and six fatigue tests undertaken as part of this research program. Each test is briefly summarized, including key observations during loading, peak loads and deflections, image correlation data where relevant, and discussions and photos of failure modes. Discussion and comparison of these results take place in a subsequent chapter.

4.1 Static Testing Program Results

A total of six specimens were tested as part of the static testing program. Of these, three were from Bridge No. 810003 and three were from Bridge No. 910180. Table 4-1 shows a summary of the results from the static testing program, while Figure 4-1 shows the load versus deflection results. The tabulated FRP tension strain measured during testing is incremental, so measured values should be added to the initial 4100 microstrain applied at the time of strengthening (initial tension force of 18.5 kips).

Table 4-1: Static test summary

	Unstrengthened			Strengthened		
	SCU1	**SCU2**	**WCU1**	**SCS1**	**SCS2**	**WCS1***
Ultimate Load (kips):	25.8	19.8	26.5	29.0	30.9	15.6
Maximum Deflection (inches):	11.9	11.1	8.3	9.4	7.6	5.8
Incremental Measured FRP Tension Strain ($\mu\varepsilon$):	--	--	--	3205	4333	2957
Incremental Measured FRP Tension Force (kips):	--	--	--	14.5	19.5	13.3
Failure Mode:	CC	CC	CC	CC, LS/R	LS/R	CC

Note: CC = Concrete Crushing; LS = Concrete Longitudinal Splitting; R = FRP Rupture
* MF-FRP applied to one stem only

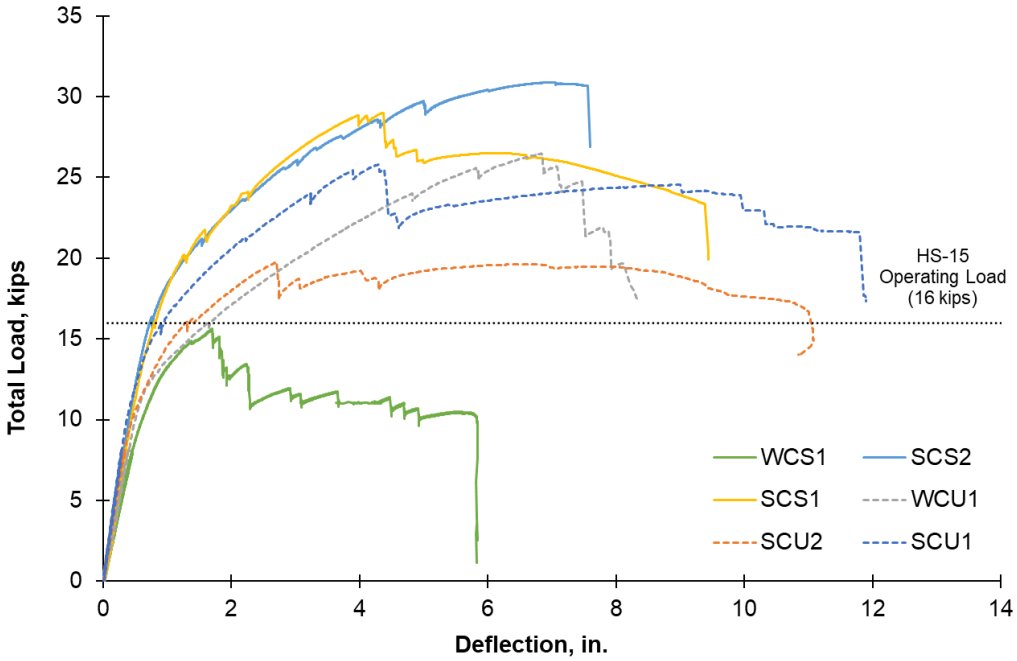

Figure 4-1: Load versus midspan deflection behavior for six static tests

*MF-FRP applied to one stem only on WCS1

4.1.1 Unstrengthened Control Specimens

Specimen SCU1 failed at a peak applied load of 25.8 kips and corresponding deflection of 11.9 in. During testing, the specimen experienced minor concrete spalling and heavy crack formation, as well as rupture of the bottom prestressing strand. The primary mode of failure for this specimen was concrete crushing, which occurred at the top mid-span section. The failure mode of the specimen is shown in Figure 4-2.

Figure 4-2: Specimen SCU1 at failure

Specimen SCU2 failed at a peak load of 19.8 kips with a corresponding maximum vertical deflection of 11.1 in. During testing, the specimen experienced significant concrete spalling and cracking. The failure mode for this specimen was concrete crushing at the top mid-span section, as shown in Figure 4-3.

Figure 4-3: Specimen SCU2 at failure

Specimen WCU1 failed at a peak load of 26.5 kips with a maximum corresponding deflection of 8.32 in. During testing, the beam experienced concrete cracking, concrete spalling, and rupture of the bottom prestressing strand in both stems. The load dropped after each strand rupture; however, the beam recovered and the applied load increased with increasing displacement. The primary failure mode for this specimen was crushing of concrete at the top mid-span section, as shown in Figure 4-4. The load did not increase after concrete crushing initiated, confirming this was the controlling failure mode.

Figure 4-4: Specimen WCU1 at failure

4.1.2 Strengthened Specimens

Specimen SCS1 failed at a peak load of 29.0 kips with a maximum vertical deflection of 9.44 in. During testing, the specimen experienced concrete spalling and prestressing strand rupture. The bottom right prestressing strand exhibited a wire rupture at an applied load of 21 kips. After that, more wires ruptured as the prestressing strands relaxed, but the load climbed steadily to the peak load. At the peak load, the bottom right prestressing strand completely ruptured. Substantial concrete spalling from the left stem also occurred at this point. The load dropped to 26.5 kips as the concrete at the top midspan section started to crush. The load began to slowly decrease as deflection increased. At 23 kips and over 9 inches of deflection, the MF-FRP plate on the right side of the beam ruptured, ending the test. Images of the tested specimen are shown in Figure 4-5.

Figure 4-5: Images of SCS1 at failure

The development of failure in the FRP strap of Specimen SCS1 may be seen in Figure 4-6, which highlights the principal tensile strains in the strap as captured by the image correlation system at the peak load immediately prior to failure. The snapshots shown are labeled LS1, LS2, and LS3, which are snapshots taken seconds apart to demonstrate the propagation of failure in the FRP strap. At an applied load of 26.2 kips, the development of tensile strains is evident at each bolt location, with a crack forming along the right side of the bottom row. This results in a drop in sustained applied load to 25.1 kips, at which point the propagation of the bottom row crack is observed. Applied load continues to drop as deflections increase, and at an applied load of 23.1 kips, longitudinal splitting along both the top and bottom row of bolts is evident, with the crack unzipping to the end of the plate, triggering final failure of the test specimen.

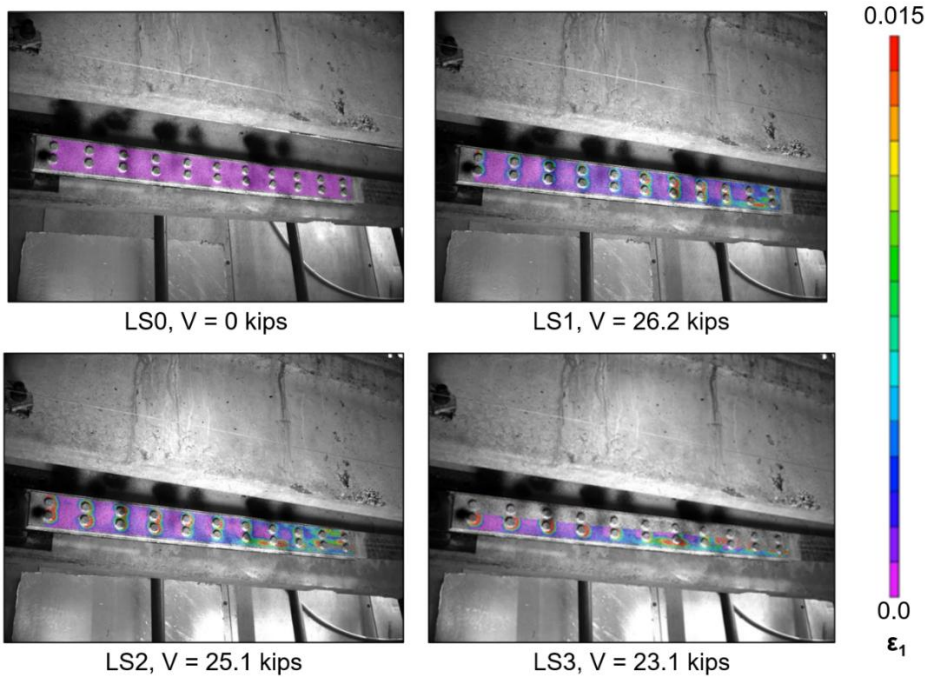

Figure 4-6: Principal tensile strains of SCS1

Specimen SCS2 failed at a similar peak load to Specimen SCS1 at 30.9 kips with a maximum deflection of 7.64 in. The specimen exhibited cracking, longitudinal splitting, and spalling of the concrete of both stems during the test. The specimen sustained a load of 29.7 kips when the left MF-FRP plate developed a significant longitudinal crack that propagated along the line of the initial crack. The load continued to increase slightly from this point, peaking immediately before the left MF-FRP plate ruptured, ending the test, as shown in Figure 4-7.

Figure 4-7: Specimen SCS2 at failure

Specimen WCS1 failed at a peak load of 15.6 kips with a corresponding maximum deflection of 5.84 in. As a result, this specimen did not achieve the HS-15 operating load of 16 kips. The specimen experienced cracking and spalling of concrete throughout the test. At the peak load, significant concrete spalling was observed. This heavy spalling correlated with a drop in load capacity that continued until the midsection of the beam ultimately crushed, resulting in the catastrophic failure shown in Figure 4-8. However, after inspection, the MF-FRP system on the repaired stem remained intact, indicating that failure was heavily influenced by the unstrengthened stem. During the test, stress on the unstrengthened stem was observed as greater vertical deflection relative to the repaired stem during loading, and a torsion of the specimen towards the unstrengthened stem was evident near and at failure.

Figure 4-8: Images of WCS1 at failure

4.2 Fatigue Testing Program Results

4.2.1 Static Proof Testing Results

Table 4-2 shows a summary of the results from the static proof tests, conducted prior to corresponding fatigue tests, with Figure 4-9 showing the load-deflection results. Data from each proof test at key points during loading are presented in this section, including observations, measured data, and failure modes. Discussion and comparison of these results are presented in a subsequent chapter.

Table 4-2: Static proof test summary

	Strengthened				Unstrengthened	
	WCS2*	**SCS3**	**WCS3**	**SCS4****	**SCU3**	**SCU4**
Max. Load, kips	10.8	16.3	16.3	16.2	16.2	16.2
Max. Deflection, in.	3.35	0.72	0.83	0.58	1.04	0.84
Failure Mode	PSR	None	None	None	None	None

Note: PSR = Prestressing strand rupture; *Only one stem strengthened; **Strengthened in the laboratory

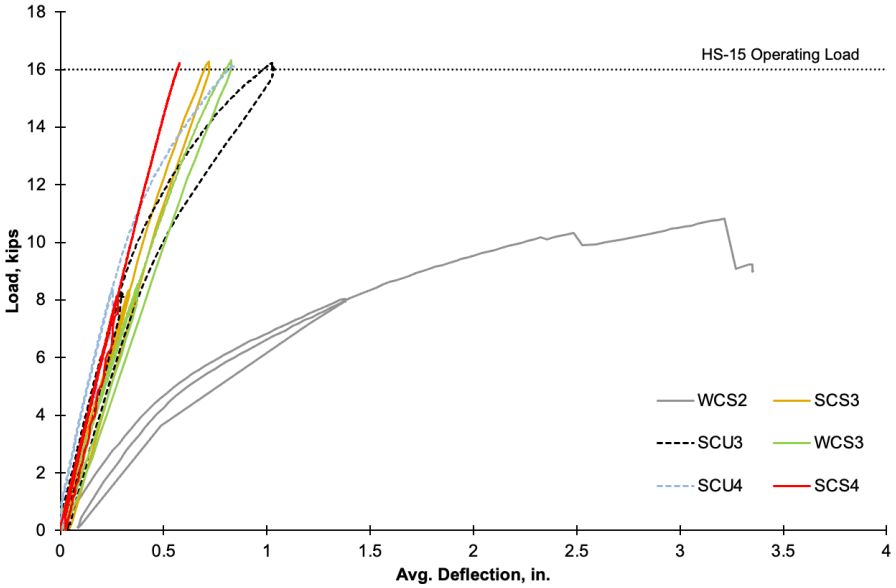

Figure 4-9: Load versus deflection graph for static proof tests

WCS2 was the first static proof test performed; recall, this member only had one stem strengthened. As mentioned in Section 3.4.4, the as-received condition of this beam, judged by visual inspection, was poor. As shown in Figure 4-9, WCS2 did not reach the operating load of 16 kips. WCS2 failed due to rupture of the bottom right prestressing strand in the unstrengthened stem (see Figure 4-10) at a maximum applied load of 10.8 kips with a corresponding maximum deflection of 3.35 in. As it is unlikely the unstrengthened stem was in such bad condition at the time of the retrofit, this finding confirms deterioration of the concrete section continued throughout the 2-year service life of the retrofit.

Figure 4-10: WCS2 bottom right prestressing strand rupture

The remaining five static proof tests, however, did achieve the HS-15 operating load of 16 kips, making them viable candidates for fatigue testing. Specimens SCS3, WCS3, and SCS4 all exhibited linear responses throughout loading to this operating load level. Specimens SCU3 and SCU4, both unstrengthened, exhibited some softening in the later stages of the static proof test load-displacement domain, with these specimens exhibiting maximum deflections of 1.04 and 0.84 in. at the maximum 16 kip load level, respectively.

4.2.2 Fatigue Testing Results

As mentioned in the previous section, WCS2 was unable to resist the operating load condition and hence, was not subjected to fatigue loading. The remaining five test specimens were loaded in fatigue for up to 250,000 cycles each and for at least 200,000 cycles each, with each cycle loading to 16 kips at midspan and then fully unloading. This section will highlight the response of the five test specimens to fatigue loading with discussion and comparison of those results in the next chapter.

Specimen SCU3 (Unstrengthened)

The 0-to-16-kip load was applied to unstrengthened specimen SCU3 101,311 times prior to failure. The total testing time was approximately 84 hours at a frequency of 0.33 Hz. Throughout the test, load and deflection data were monitored and recorded at intervals to record changes in stiffness and incremental displacement. Figure 4-11 shows the load-displacement response with increasing cycles for Specimen SCU3; the figure shows that, even at a cycle count of 541, the unstrengthened member was exhibiting nonlinearity in the load-displacement domain. With increasing cycles, both the initial stiffness as well as the overall load-displacement response of the member softened. Cycles were ultimately stopped at a count of 101,311 due to increasing deflections and the inability of the softened member and available loading equipment to achieve the fatigue load within a reasonable cycle period. Relative deflection at the midspan was roughly 2 in. at the time cycling was terminated. Note that "relative deflection" or "relative displacement" are used interchangeably from this point forward to mean the deflection that occurred within a given cycle, taking the deflection at the unloaded starting point of that cycle as zero.

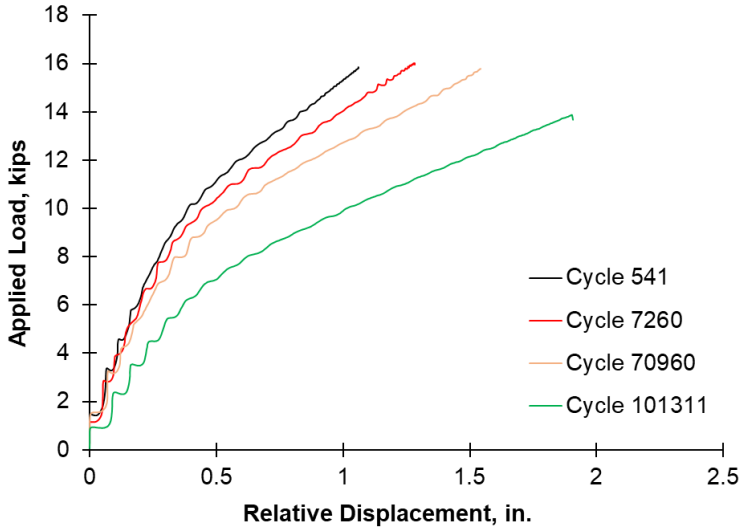

Figure 4-11: SCU3 load-displacement response with increasing cycles

Figure 4-12 shows the specimen at various stages during cycling. Even during the initial stage of 500 cycles, flexural cracks were observed in the specimen near midspan; these cracks were observed to widen and narrow as the cyclic load was applied and released. At a cycle count of approximately 20,750, damage to the exposed corroded bottom strand was observed to have section loss once the concrete encasing it near the supports had spalled off. At a cycle count of approximately 41,100, additional cracking in the section was observed; flexural cracks near midspan were evident, as well as longitudinal cracking and concrete spalling that exposed corroding strand.

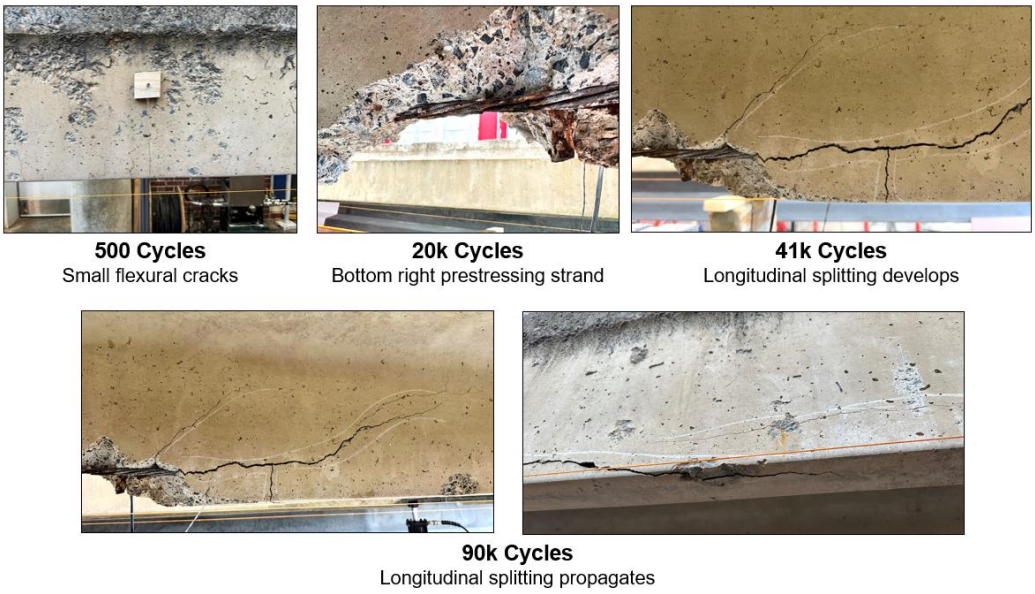

Figure 4-12: Images of SCU3 at various stages of loading.

Between cycle counts of 62,600 and 90,020, the longitudinal splitting along the ruptured corroded strand continued to develop, extending and widening near the support. Cycles were ultimately stopped after 101,311 cycles due to spalling of the concrete along the bottom of the left stem. At this load level, significant extension and propagation of the longitudinal splitting crack on the right stem developed, with the horizontal extension of the crack widening significantly in the vicinity of the location of strand rupture.

After the cyclic tests were completed, the member was then tested to failure statically to determine its residual capacity. The load-displacement response of the member is shown in Figure 4-13. The member ultimately failed due to rupture of the prestressing strand in the left stem at a load of 22.5 kips; an image of the member at failure is also shown in Figure 4-13.

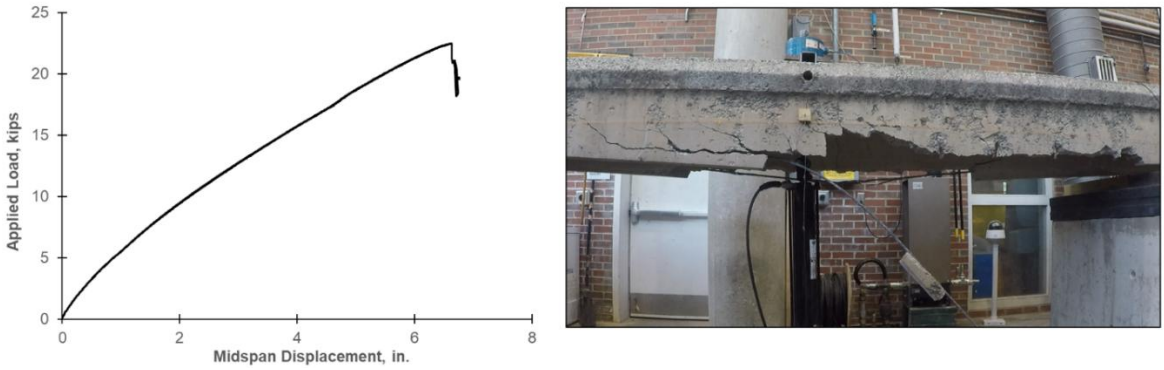

Figure 4-13: Load-displacement response and image of SCU3 at failure

Specimen SCU4 (Unstrengthened)

The 0-to-16 kip cyclic load was applied to specimen SCU4 152,160 times. The total testing time was approximately 148 hours at a frequency of 0.30 Hz. Throughout the test, load and deflection data were monitored and recorded at intervals to record changes in stiffness and relative displacements. Figure 4-14 shows the load vs. relative displacement response with increasing cycles for Specimen SCU4. From the beginning of the cyclic program, the member exhibited a nonlinear load-deflection response. As cycles were continuously applied, the maximum midspan deflection of the member increased, and the maximum

load it could sustain within the predetermined cycle frequency decreased. The test was concluded once it was observed that the member with degraded stiffness was no longer able to achieve the 16-kip applied load with available equipment at a realistic rate of loading and without significant deflection. Relative deflections ranged from approximately 0.90 in. at 50 cycles to 1.43 in. at 152,160 cycles.

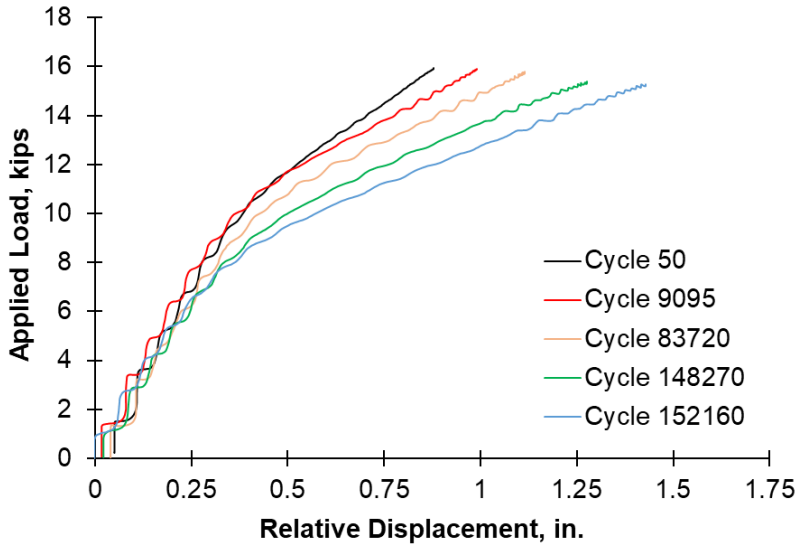

Figure 4-14: Load-displacement response of SCU4 with increasing cycles

Figure 4-15 shows the member in its initial condition and at 148,250 cycles. The member did not exhibit significant signs of distress until approximately 148,250 cycles, at which point concrete spalled from the left stem, exposing the bottommost strand; the strand did not show signs of corrosion. As load was continuously applied, the response of the member continued to soften, prompting the conclusion of fatigue cycles.

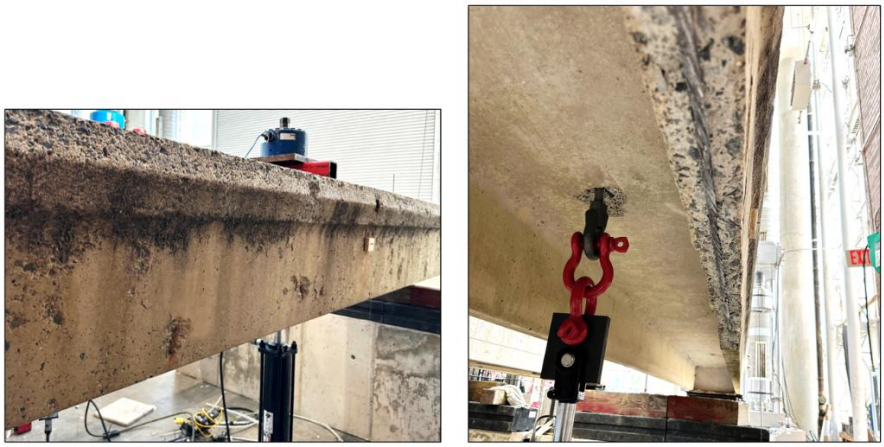

Figure 4-15: Images of SCU4 at various stages of loading

After concluding the cyclic portion of the testing, the member was then tested statically to failure. The member failed at an applied load of 27.7 kips due to rupture of the bottommost strand in the left stem. An image of the member at failure is shown in Figure 4-16, along with the load-displacement response.

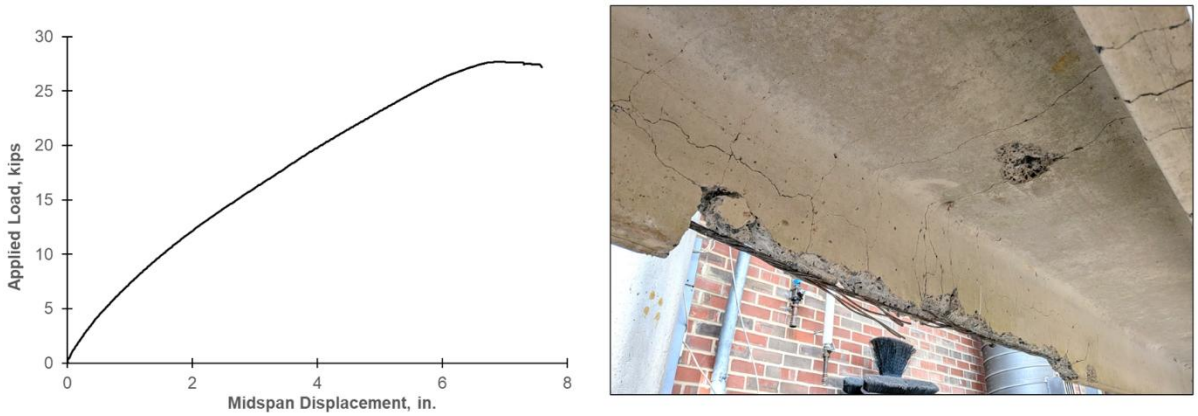

Figure 4-16: Load-displacement response and image of SCU4 at failure

Specimen SCS3 (Strengthened)

Specimen SCS3 failed after 200,200 cycles of the 0-to-16-kip fatigue load. The total testing time was just over 168 hours at a frequency of 0.33 Hz. Throughout the test, load and deflection data were monitored and recorded at intervals to record changes in stiffness and incremental displacement. Figure 4-17 shows the load-displacement response as the cycle count increased. For cycles up to 160,000, the midspan deflection was consistent and the stiffness of the specimen was generally linear with only minor degradation. Cycles after the 160,000-mark showed higher deflections, signifying that the concrete section was softening, and the stiffness was decreasing significantly and exhibiting nonlinearity. As the cycle count increased, the deflection started to increase rapidly, with the specimen reaching a maximum relative deflection of 4.5 in.

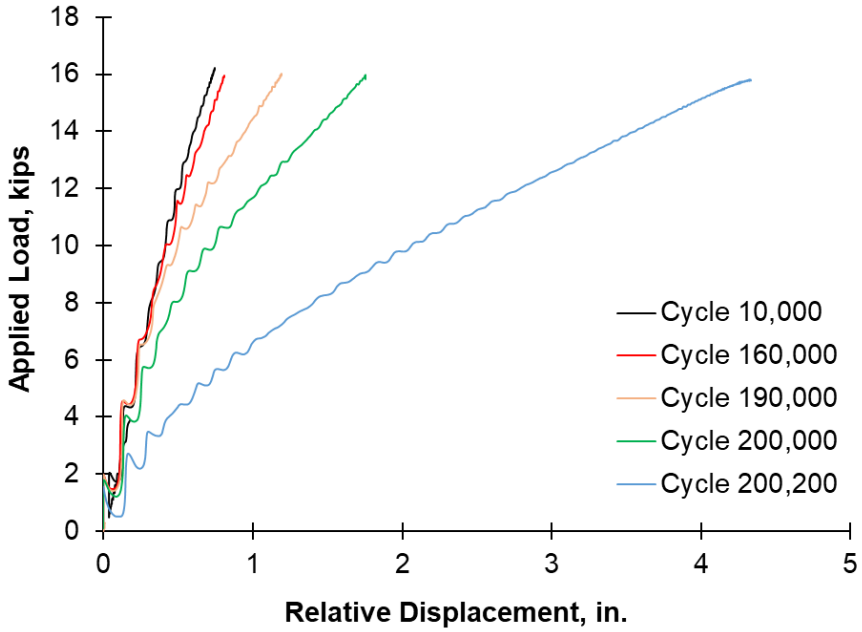

Figure 4-17: SCS3 load-displacement response with increasing cycles

Figure 4-18 shows the specimen at various stages during cycling. From cycles 10,000 to 20,000, small flexural cracks started to form, stemming from existing areas of degraded concrete. Between cycles 80,000

and 120,000, substantial concrete spalling developed, with small concrete chunks falling off each stem. Between cycles 120,000 and 160,000, concrete chunks continued to spall off, exposing the bottom prestressing strand on the right stem. This strand had experienced some prior corrosion, which was visible after the concrete spalled off.

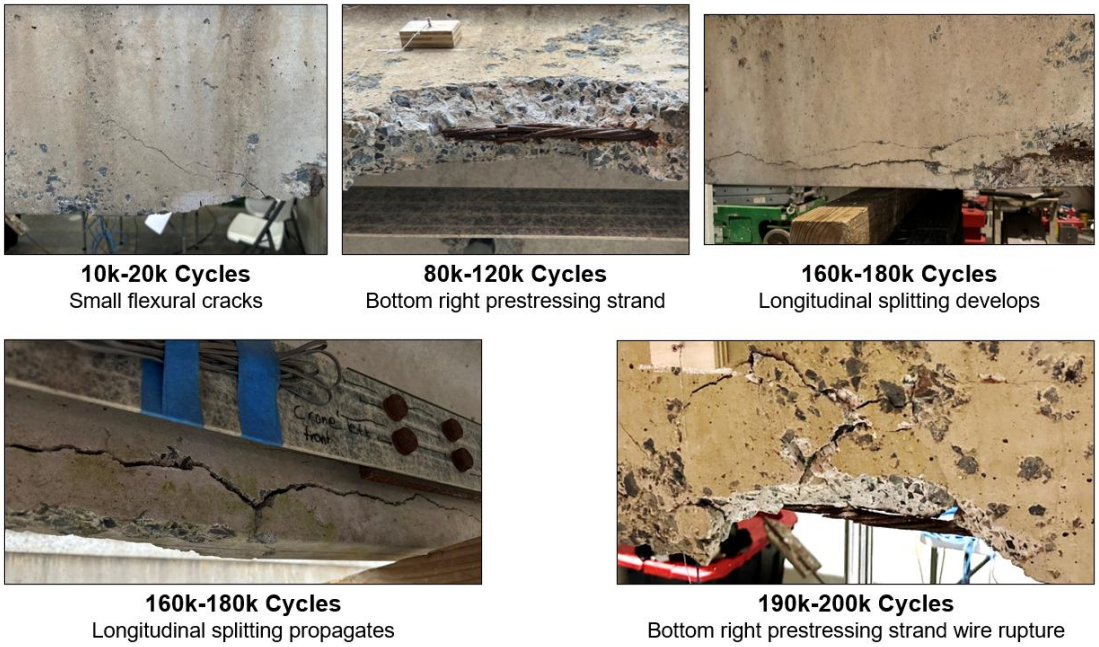

Figure 4-18: SCS3 at various stages of cycling.

Between cycles 160,000 and 180,000, existing flexural cracks propagated, and longitudinal splitting was observed along the concrete at the bottom layer of the prestressing strand. Between cycles 180,000 and 190,000, the longitudinal splitting propagated, and concrete chunks continued to spall off. From cycles 190,000 to 200,000, concrete spalling, flexural crack propagation, and longitudinal splitting continued to develop and expand. In addition, the bottom right 7-wire prestressing strand had several wires rupture. Between cycles 200,000 and 200,200, major concrete spalling along both stems occurred. This spalling exposed the bottom prestressing strand on the left stem and the higher three prestressing strands on the right stem. Concrete spalling and longitudinal splitting continued until the top three prestressing strands in the right stem ruptured (shown in Figure 4-19), ending the test at 200,200 cycles. Note that while the member had not collapsed at the end of fatigue cycling, because of the severe degradation in the last few cycles, this member was not tested statically to failure.

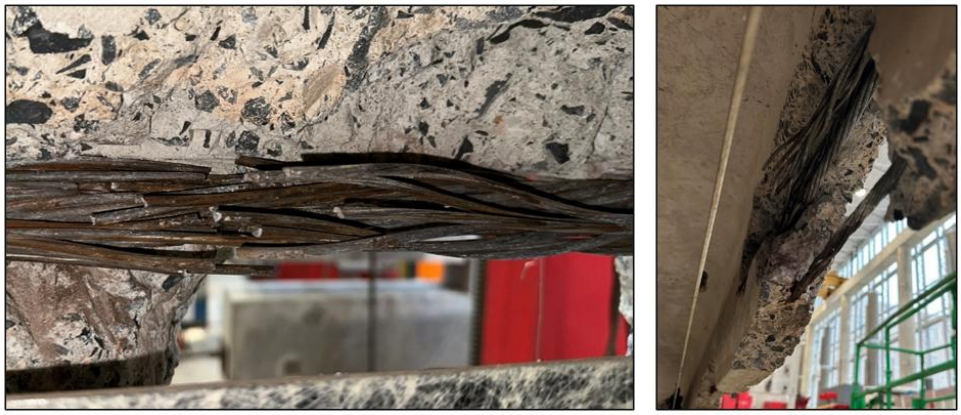

Figure 4-19: SCS3 at the end of fatigue testing.

Specimen WCS3 (Strengthened)

The 0-to-16 kip cyclic load was applied to specimen WCS3 238,732 times. The total testing time was approximately 201 hours at a frequency of 0.33 Hz. Throughout the test, load and deflection data were monitored and recorded at intervals to record changes in stiffness and incremental displacement. Figure 4-20 shows the load-displacement response with increasing cycles for Specimen WCS3. Initially, the member exhibited a linear elastic response. The response then showed increasing nonlinearity as the cyclic load was applied, with peak relative displacements beginning at approximately 0.75 in. at 541 cycles and ending at approximately 1.5 in. at 238,732 cycles. The test was concluded upon reaching the target number of cycles.

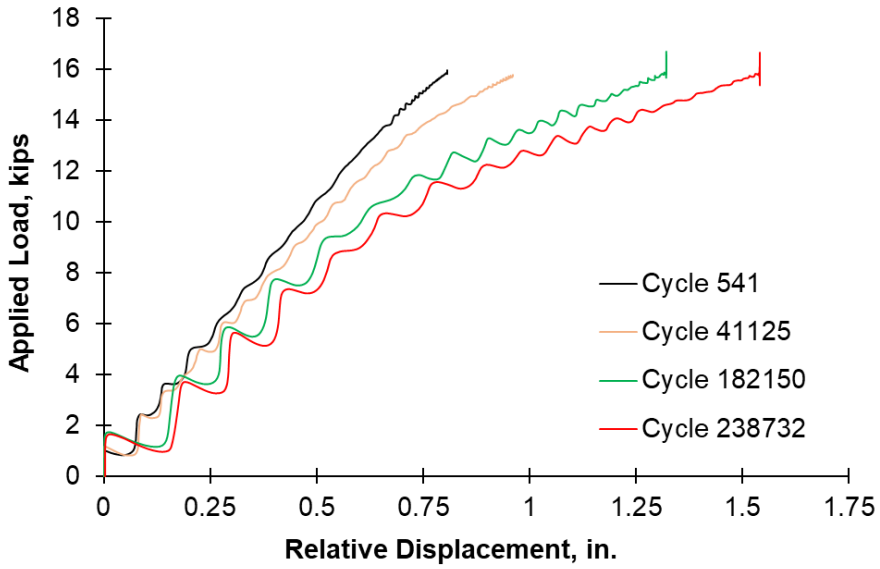

Figure 4-20: WCS3 load-displacement response with increasing cycles

Figure 4-21 shows the member at various stages of this fatigue program. At the 541 cycle mark, the member was relatively unchanged from its initial condition; concrete spalling was present on the left stem at midspan exposing corroded strand, and longitudinal cracks were evident near the supports. At a cycle count of 1,660, spalling was observed on the right stem, exposing more corroded strand at midspan. At a cycle count of 20,757, concrete spalling was observed on the left stem at midspan, further exposing the bottommost corroded strand. At a cycle count of 41,101, it was observed that wires of the corroded strand had ruptured on the left stem of the member. The member then remained relatively unchanged until the end of the cycle program.

Figure 4-21: Images of WCS3 at various stages of loading

At approximately 238,000 cycles, cracks began to form around the bolts anchoring the strengthening assembly to the beam in a pattern that suggested a block shear-type failure. The damage was particularly pronounced at the end that housed the turnbuckle of the strengthening system. At both ends, however, longitudinal splitting cracks were observed to extend from the bolted connections towards midspan. Additionally, further concrete spalling was observed on the right stem at midspan. This rapid overnight degradation suggested that the member was approaching the end of its load-carrying capacity so cycling was stopped for a static test to failure.

After the cyclic tests were completed, the member was then tested to failure statically to determine its residual capacity. The load-displacement response of the member is shown in Figure 4-22. The member ultimately failed due to block shear of the bolted connection at an applied load of 23.4 kips; an image of the failure mode is also shown in Figure 4-22.

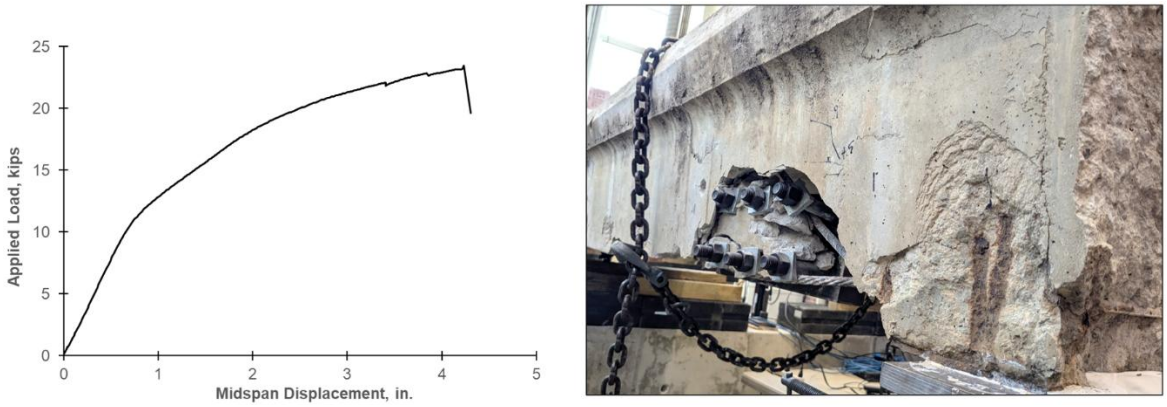

Figure 4-22: Load-displacement response and image of WCS3 at failure.

Specimen SCS4 (Strengthened in the Laboratory with new MF-FRP)

The 0-to-16 kip cyclic load was applied to specimen SCS4 250,000 times. The total testing time was approximately 243 hours at a frequency of 0.30 Hz. Throughout the test, load and deflection data were monitored and recorded at intervals to record changes in stiffness and incremental displacement. Figure

4-23 shows the load-displacement response with increasing cycles for Specimen SCS4. Throughout the fatigue cycling program, the response of the member remained in the linear-elastic range, with linearity observed up to 250,000 cycles. Recall, this member was strengthened in the laboratory with new MF-FRP so the retrofit system did not undergo cycles in the field.

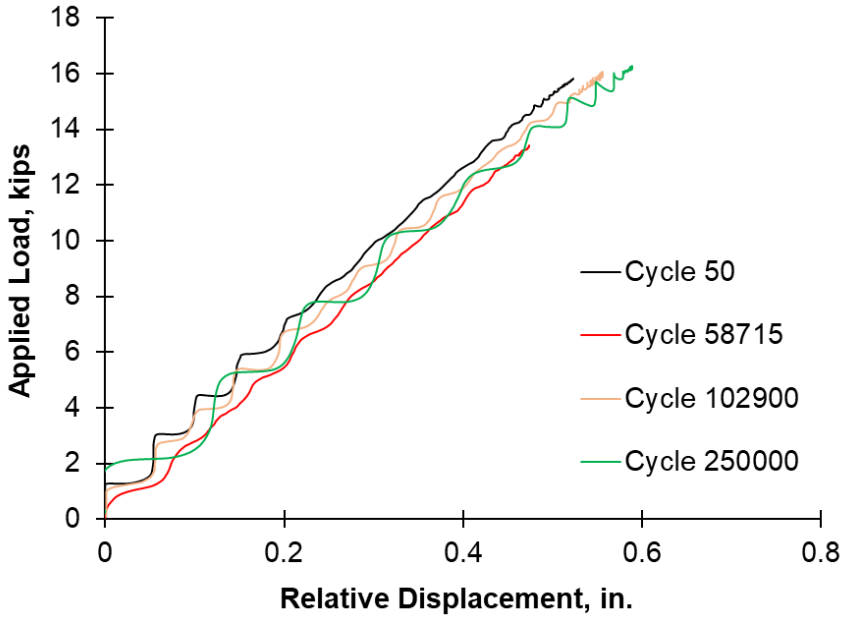

Figure 4-23: Load-displacement response of SCS4 with increasing cycles

Figure 4-24 shows images of the FRP strap at various stages of loading. At approximately 30,525 cycles, hairline cracks were observed around the bolt holes in the FRP strap; these cracks measured about 1 in. in length. At 76,848 cycles, these cracks had, in some cases, extended slightly to approximately 2 in.; in other cases, the cracks remained unchanged. The member appeared to otherwise have experienced no degradation until 250,000 cycles.

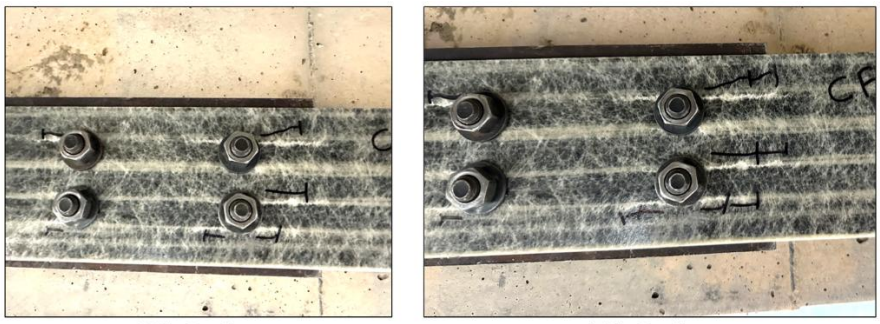

Figure 4-24: Images of the FRP straps on SCS4 at various stages of loading

The member was then tested to failure at the completion of the fatigue program. Specimen SCS4 achieved a maximum capacity of 37.0 kips; the member ultimately failed due to rupture of the right FRP strap; further loading resulted in rupture of the left strap, as well as crushing of the concrete top flange. Figure 4-25 shows an image of the member at failure, as well as the load-displacement response.

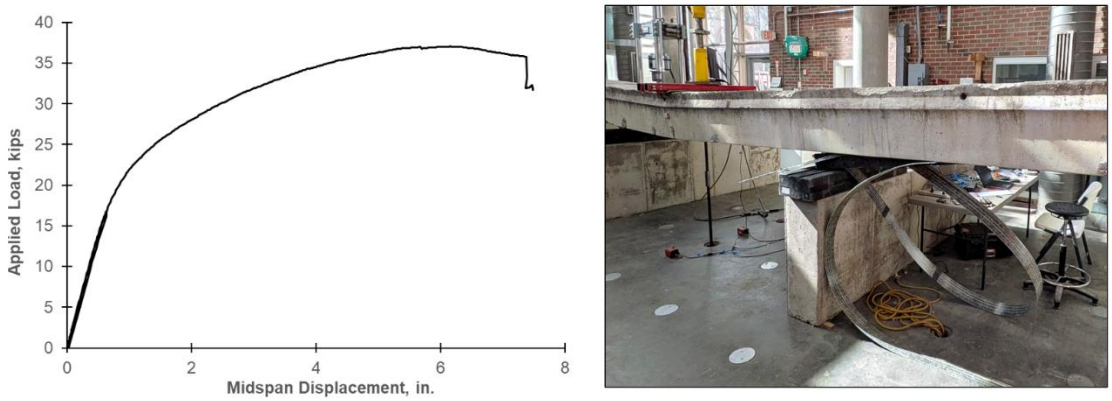

Figure 4-25: Load-displacement response and image of SCS4 at failure

5 Analysis of the Experimental Results

This chapter presents an analysis of the results presented in Chapter 4, including the static testing program, the fatigue testing program, and the material testing program. In addition, the opportunity to implement the MF-FRP system on more bridges throughout North Carolina is actively being pursued. Two candidate bridges have been analyzed, and one is currently in the process of having the MF-FRP retrofit system installed. The condition and analysis of these bridges are also presented in this chapter.

5.1 Static Testing Program Analysis

Results from the static testing program were primarily positive, as all specimens except for one exceeded the original operating load level. Table 5-1 shows the percentage of the original operating load of 16 kips that was sustained for the static testing program specimens. Specimen WCS1, with heavy degradation in the non-strengthened stem, reached 98% of the operating level.

Table 5-1: Percent increase from HS-15 operating load

	Unstrengthened			Strengthened		
	SCU1	**SCU2**	**WCU1**	**SCS1**	**SCS2**	**WCS1***
Avg. Concrete Compressive Strength, psi	7840	7500	4310	7680	6950	4860
HS-15 Operating Load, kips	16.0	16.0	16.0	16.0	16.0	16.0
Ultimate Load at Static Failure, kips	25.8	19.8	26.5	29.0	30.9	15.6
% of HS-15 Operating Load	161	124	166	181	193	98

* Only one stem strengthened

The unstrengthened control specimens SCU1, SCU2, and WCU1 performed well, showing load-carrying capacities of 161%, 124%, and 166% of the 16-kip operating load, respectively. These specimens did not have the MF-FRP retrofit system installed, as they were selected from a collection of girders removed from their respective bridges that were not repaired in the field due to their reasonably sound condition. The initial condition of specimens SCU1 and WCU1 showed no visible signs of the types of damage that would generally indicate an inability to carry the required operating load. Specimen SCU2 did exhibit some light section loss on the right stem's locally exposed bottom prestressing strand. Even with this damage, the specimen still achieved and surpassed the required operating load. This result established a baseline for the rest of the static tests, as the retrofitted specimens would ideally achieve a load-carrying capacity equivalent to that of the less degraded non-retrofitted specimens, and at least the original operating load. The concrete compressive strength of specimen WCU1, lower than the original 5.0 ksi design strength specified, indicated a potential concern compared to the other specimens, as weaker concrete often indicates greater porosity and more extensive corrosion. However, the flexure test results indicated that WCU1 performed the best of the unstrengthened specimens, indicating that concrete compressive strength alone, as indicated by cores, cannot accurately predict flexural performance.

Retrofitted specimen SCS1 performed well, showing an increase in load-carrying capacity of 81%, over the operating load, which is better than all control beams tested, despite the extensive underlying damage in SCS1 that triggered the retrofit. In addition to longitudinal MF-FRP, this specimen was repaired with the optional steel shear strengthening plates in one end region. The end region with the shear-strengthening plates exhibited no damage during the test, suggesting adequate performance of the bolted-on shear repair.

Retrofitted specimen SCS2 also performed well, showing an increase in load capacity of 93% over the original operating load. This load was higher than any of the control beams tested, indicating the strengthening system performing as intended. Notably, this specimen had extensive damage to the MF-FRP plate prior to testing, shown in Figure 5-1, that was likely created during demolition of the bridge. It was suspected that this heavy damage would decrease the capacity of the beam by causing the retrofit system to fail prematurely; however, this specimen performed the best of all static specimens. It is thus concluded that the roughly 30% reduction in cross-sectional area along nearly the full length of FRP (damage prior to

receiving the specimen at the laboratory) did not degrade system performance because: 1) this damage did not extend past the first line of bolts at each end of the FRP plate; and 2) the section lost to damage, while extensive, was comparable to the reduced cross-sectional area at any pair of bolts along the bolted interface between steel plate and FRP plate. The length of the bolted connection was sufficient to distribute the tension force around the damaged area of the FRP plate, overcoming any effects of shear lag, and providing confidence in the robustness of the bolted MF-FRP system.

Figure 5-1: FRP plate damage prior to testing in SCS2

Moving to specimen WCS1 with strengthening on one stem only, WCS1 was the only specimen that did not achieve the original operating load, falling short by 2%. After the proof test concluded in failure of the specimen, the specimen was secured and inspected for indications of why an early failure occurred. After inspection, it was found that the internal prestressing strands of the unstrengthened stem were corroded and had experienced significant section loss. Figure 5-2 shows the initial condition of the unstrengthened stem and, aside from a few minor flexural cracks, the concrete appeared to be in good condition. However, Figure 5-3 shows a close-up photo of the internal prestressing strands inside the unstrengthened stem, revealing that the bottom strand was fully corroded and had separated at mid-span. The top three strands were also fully corroded and broken at mid-span. After this inspection, it was concluded that the cause of failure was the insufficient load-carrying capacity of the internal prestressing strands on the unstrengthened stem. This result is concerning, as it demonstrates the potential for significant internal damage not reflected by the external visual condition of the beam.

Figure 5-2: WCS1 unstrengthened stem initial condition

Figure 5-3: WCS1 internal prestressing strand corrosion

Comparing the results from the static testing program to those of (McCoy, 2019) and (Lin, 2021), the behavior of the control and strengthened specimens performed similarly. When compared to the control specimens (one damaged and one undamaged C-channel beam) tested by (McCoy, 2019), specimens SCU1, SCU2, and WCU1 exhibited similar results. The undamaged specimen from (McCoy, 2019) reached a peak load of 29.6 kips, while the damaged specimen reached a peak load of 18.8 kips. Unstrengthened (and visually undamaged) SCU1 and WCU1 reached peak loads of 25.8 and 26.5 kips, respectively. Damaged and unstrengthened Specimen SCU2 had the bottom prestressing strand exposed in one stem (see the condition assessment in Chapter 3), and reached a peak load of 19.8 kips, comparable to the damaged specimen tested by (McCoy, 2019). Overall, the results from the control specimens of this testing program were consistent with previous control tests. This result may be considered somewhat surprising in that the recently tested beams are six years older than the McCoy specimens and have the same specified concrete strength, prestressing strand layout, and ultimate prestressing force. However, the recently tested channel beams, on average, exhibited similar capacities to those tested six years prior that were of a similar age, from similar bridges, and exposed in similar environments. As such, degradation is not simply a function of structure age, but is very site-specific and likely even beam specific.

(McCoy, 2019) and (Lin, 2021) also tested a total of five strengthened C-channel specimens in flexure. (McCoy, 2019) tested two undamaged specimens that were retrofitted with the MF-FRP system. These tests reached a peak load of 35.1 and 37.3 kips, respectively. (McCoy, 2019) also tested two damaged specimens that were retrofitted with the MF-FRP system. These tests reached peak loads of 27.6 and 26.1 kips, respectively. (Lin, 2021) tested one damaged, strengthened specimen that reached a peak load of 27.1 kips. In the current work, damaged and strengthened specimens SCS1 and SCS2 reached peak loads of 29 and 30.9 kips, respectively. When compared to the previous tests performed on damaged specimens with the MF-FRP retrofit system installed, the test results from the current research are similar, once again proving the ability of the system to restore the candidate specimen to its original inventory and operating load capacities. Importantly, the current results indicate that the field-observed damage present in the beams tested is no worse than the damage intentionally induced in some of the beams tested by McCoy and Lin. As such, prior results achieved on specimens with laboratory-induced damage are applicable and conservative to common field situations.

5.1.1 LSA Prediction and Experimental Results Comparison

The layered section analysis (LSA) developed by (Bourara, 2019) and (Lin, 2021) was utilized in the current research to predict the capacity of the specimens tested. Table 5-2 shows the peak load from the current experimental tests, the LSA prediction, and the ratio of the prediction to the experimental value.

Table 5-2: LSA versus experimental ultimate load

	SCU1	SCU2	WCU1	SCS1	SCS2	WCS1
Experimental Ultimate Load (kips)	25.8	19.8	26.5	29.0	30.9	15.6
LSA Analysis Ultimate Load (kips)	29.0	20.0	28.5	27.3	27.3	25.4
LSA/Experimental	1.12	1.01	1.08	0.94	0.88	1.63

The LSA moderately overpredicted the capacity of two unstrengthened specimens, SCU1 and WCU1, which did not have any visible significant section loss in the prestressing strands. However, there was other damage in these beams (spalling) as noted in Section 3.4.2. LSA predictions did not consider any damage for these specimens, so their actual and aged condition may explain why they both underperformed the LSA model.

The LSA predicted the capacity of the damaged control specimen SCU2 accurately (within 1% of the experimental results), and the prediction in this case included a level of damage, estimated from the visual condition of the member. This result provides confidence in the ability of the LSA to accurately capture the ultimate capacity of specimens that have damage to their prestressing strands, assuming an accurate estimation of that level of damage can be included in the LSA modeling.

The LSA underpredicted the capacity of two strengthened specimens SCS1 and SCS2 by a modest margin. The LSA is generally conservative in its predictions involving the MF-FRP system due to conservative assumptions about MF-FRP bolted capacity and stiffness. This moderately conservative prediction is generally desirable, and it should help provide confidence to designers when implementing the MF-FRP repair system on candidate specimens.

More troubling is that the LSA significantly overpredicted the capacity of Specimen WCS1, the specimen that failed suddenly and unexpectedly in its one unstrengthened stem. As mentioned in Section 3.4.2, this specimen had extensive internal damage to the prestressing strands that was not initially visible, causing a premature, sudden failure in this stem. As such, the prediction from the LSA, which assumed no section loss in these strands, is not valid for this specimen, as the initial zero-damage assumption was incorrect.

5.2 Fatigue Testing Program Analysis

5.2.1 Static Proof Testing Analysis

Results from the initial static proof tests on fatigue specimens were mixed. Five specimens were able to achieve the 16-kip operating load without issue and were thus subjected to the fatigue testing. Specimen WCS2, however, did not reach the 16-kip operating load, and it was therefore not possible to subject this beam to the planned fatigue testing. This failure, however, was not entirely unexpected. Like specimen WCS1, WCS2 only had the MF-FRP repair applied to one stem. The unstrengthened stem did have the bottom prestressing strand exposed, and this strand was also heavily corroded. A patch had previously been installed in the field after significant spalling had occurred, illustrating the potential risk of patching over corroded prestressing, or of the patching materials allowing corrosion to continue. Even so, as described in the report on the initial condition of WCS2, the bottom prestressing strand appeared intact and tensioned. Failure of the specimen involved rupture of this bottom prestressing strand in the unstrengthened stem, and demonstrated the strand had experienced heavy corrosion and was rendered insufficient to carry the operating load. While strengthening only a single stem is efficient in the field, a key recommendation from this research is to always strengthen both stems of a damaged channel member, as visible damage in one stem indicates likely damage in the other, even if that damage is not visually obvious.

5.2.2 Fatigue Testing Analysis

The results of the fatigue cycles were generally positive, highlighted in Table 5-3. In this table, the number of cycles applied to each specimen is converted to an equivalent number of years in service using the predetermined AADT and BC percentages. This equivalent number of years is then added to the prior years in service for the members that were field-strengthened with the retrofit system in order to estimate the fatigue life of the repair system. All of the members that achieved the 16-kip proof test, strengthened or not, were able to sustain at least another 100,000 cycles of loading, equivalent to approximately 1.25 years in service at the predetermined AADT and BC percentages. In general, the strengthened specimens were able to resist significantly more cycles and exhibited better performance than the unstrengthened members. Specimens SCS3, WCS3, and SCS4, sustained 200,200; 238,732; and 250,000 cycles, respectively. Unstrengthened specimens SCU3 and SCU4 were able to resist 101,311 and 152,160 cycles, respectively. Note that the retrofit system of Specimen SCS4 was not in field service for the 2 years prior to fatigue testing, as this specimen was strengthened in the laboratory. At the conclusion of testing, this member did not exhibit any nonlinearity in its load-displacement response. From this limited dataset, it may be concluded that strengthening the specimens significantly increases their fatigue life, as compared to unstrengthened specimens. Up to approximately 5 years total from the application of the strengthening in the case of WCS3.

Table 5-3: Cycles and equivalent years in service for fatigue specimens

Specimen	Cycles Applied	Static Capacity Post-Fatigue	Equivalent Years	Prior Years Retrofit in Service	Total Years Retrofit in Service
SCS3	200,200	Degraded^{+}	2.5	2	4.5
WCS3	238,732	23.4 kips	3.0	2	5.0
SCU3	101,311	Degraded^{+}	1.3	0	0
SCU4	152,160	27.7 kips	1.9	0	0
SCS4	250,000	37.0 kips	3.1	0	3.1

+Beams heavily degraded at cycle termination can be assumed to have a residual capacity less than 16 kips.

Figure 5-4 shows the degradation in flexural stiffness as a function of the number of cycles applied for all five fatigue specimens. Here, stiffness is calculated by dividing the maximum load by the maximum midspan deflection for a given cycle as a proxy for flexural distress. A lower stiffness likely indicates onset of nonlinearity or degradation in the linear-elastic response. In all cases, the strengthened specimens exhibited higher stiffnesses at a given cycle count compared to the unstrengthened specimens. However, even within the strengthened specimens, this stiffness varied significantly, highlighting the impact of individual beam condition on the effectiveness of the strengthening.

Notable is the relatively rapid degradation in stiffness, particularly in the case of SCS3; the stiffness of this member was 20 kip/in. at a cycle count of 160,000 and decreased to less than 5 kip/in. within 40,000 additional cycles (the equivalent of approximately 6 months). This degradation in stiffness was accompanied by significant flexural distress in the member, including concrete spalling and the initiation and propagation of flexural and longitudinal splitting cracks. This observation highlights the importance of continuing to regularly inspect bridges in the field that have been strengthened or that have been observed to have flexural distress, as their condition may degrade rapidly over many months. An annual inspection may be more appropriate for these heavily degraded structures rather than a biennial.

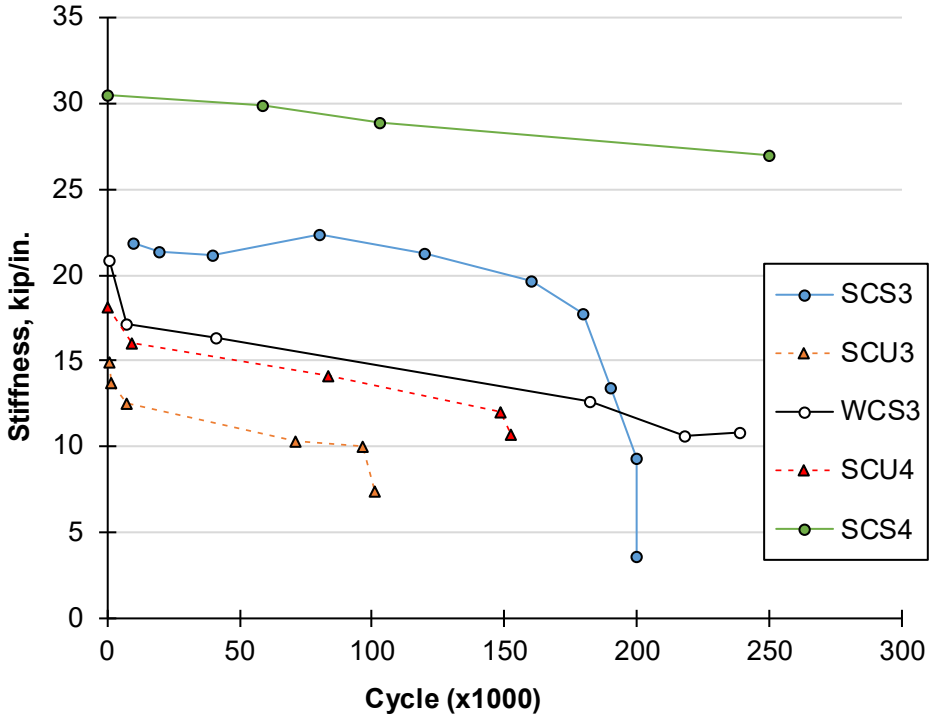

Figure 5-4: Change in stiffness with cycle count for fatigue tests

Figure 5-5 shows the typical condition of the FRP system in the three strengthened test specimens after the conclusion of the fatigue cycles. The thick black lines on the FRP system are black marker traces of hairline cracks observed in the FRP. It is clear from the images that the damage to the FRP system is minimal, and that the primary determinant of residual capacity in a strengthened channel beam is the extent of degradation in the concrete section. All three members exhibited hairline cracking in the FRP straps at the conclusion of cycling, but nothing was observed that would indicate impending loss of load-carrying capacity in the strengthening system. Instead, what is sometimes seen in the concrete at the conclusion of cycles in the strengthened members are the initiation of longitudinal web splitting cracks in the vicinity of the bolted connection, as well as degradation of the web surrounding through-bolt holes that indicate a block-shear-style failure. The experiments conducted here indicate that generally, the fatigue life of a strengthened prestressed channel beam would not typically be controlled by the MF-FRP system.

Figure 5-5: Condition of FRP straps at the conclusion of fatigue cycles

Figure 5-6 shows the load-deflection results of the static tests to failure for four specimens at the completion of the fatigue cycles. In all cases, the members were able to sustain the HS-15 operating load of 16-kips. Interestingly, strengthened specimen WCS3 failed at a lower load than unstrengthened specimen SCU4; However, it should be noted that the strengthened specimen ultimately failed due to block shear in the anchorage region after achieving 50,000 more cycles than the unstrengthened specimen, which failed by

concrete crushing in flexure. The comparison of these results highlights that, ultimately, member performance is highly dependent on the condition of the concrete section, again highlighting the need for regular inspections of aged and damaged members.

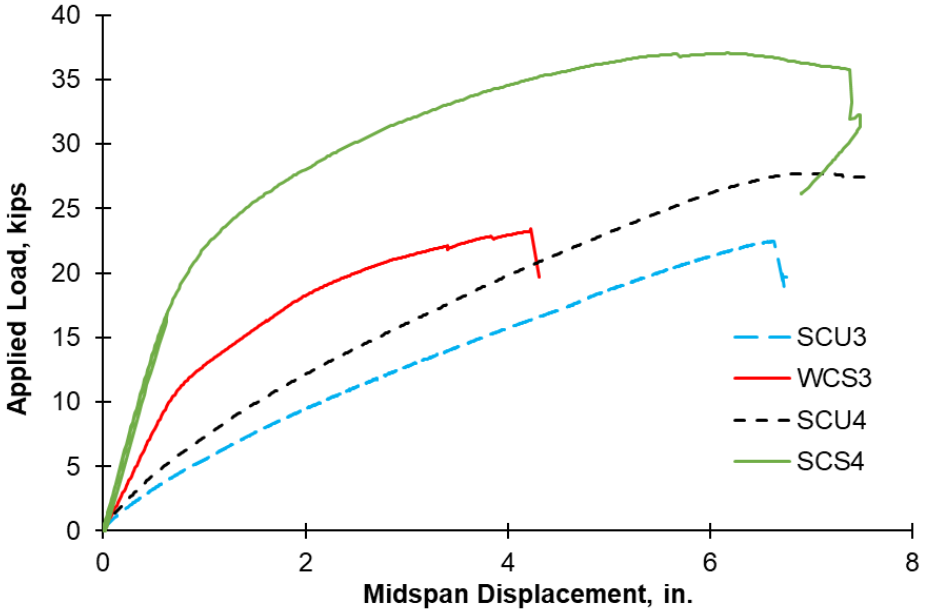

Figure 5-6: Results of static tests to failure at the conclusion of fatigue testing

Damage observed during testing to failure post-fatigue correlated with the onset of nonlinearity in the load-deflection responses included: concrete spalling around midspan, flexural cracks extending up the concrete section at midspan, and the formation of longitudinal splitting. These behaviors are all able to be readily observed in the field during routine inspections. The photos in Figure 5-7 are provided to aid in the assessment of a retrofitted specimen in the field by identifying damage consistent with the onset of load-deflection nonlinearity.

Figure 5-7: Damage signifying nonlinearity in a strengthened channel beam

5.3 Material Testing Analysis

The results from concrete material testing presented in Chapter 4 were used to assess the specimens from the two bridges. For specimens recovered from Bridge No. 810003, the specified 28-day concrete compressive strength was 5,000 psi (North Carolina DOT, 1966). However, the core compressive strength values from Chapter 4 show an increased concrete compressive strength with an average of approximately 7,460 psi. This result helped rule out that observed failure modes, such as concrete crushing, did not result from a potentially weak concrete mixture. For the concrete cores recovered from Bridge No. 910180, the specified concrete strength was unknown, but the core compressive strength values from Chapter 4 show an average strength of approximately 4,840 psi, lower than the average concrete core compression strength from Bridge No. 810003. However, specimen WCU1 (the control beam from Bridge No. 910180) had a higher load-carrying capacity than did specimens SCU1 and SCU2 (control beams) from Bridge No. 810003. Therefore, it is determined that the lower concrete compressive strength of Bridge No. 910180 did not negatively influence the test results. This finding was confirmed using the LSA tool developed by (Bourara, 2019) and (Lin, 2021), which showed similar ultimate load capacities despite differences in concrete compression strengths within the range observed from the core tests.

5.4 Analysis of Candidate Bridge for the MF-FRP Retrofit System

In addition to laboratory efforts, this research included condition assessment of a candidate bridge for MF-FRP retrofit in Bertie County, NC. Bridge No. 070018 includes a single span comprising 12 C-channel prestressed beams. One beam near mid-width is a candidate for repair with MF-FRP. Heavy corrosion is observed in the bottom strand, which is completely separated from the stem, as shown in Figure 5-8. The end region of the stem is another area of concern, as shown in Figure 5-9. Following a site visit to Bridge No. 070018, work commenced to prepare materials for a retrofit. While only one stem is damaged, materials sufficient to retrofit both stems of the beam were prepared based on the results of the current research program. A list of materials required to strengthen two stems is itemized in Appendix A.

Figure 5-8: Bridge No. 070018 with a ruptured prestressing strand

Figure 5-9: Bridge No. 070018 end region deterioration

6 Recommendations

This chapter presents recommendations related to the application and service life of the MF-FRP retrofit system. The findings from this research that support these recommendations are also summarized.

6.1 Recommendations for the Application of the MF-FRP System

Channel beams retrofitted with the MF-FRP system should always have both stems repaired, even if repair to only one stem is warranted by inspection. Test results of Specimens WCS1 and WCS2 show that if only a single stem in a channel member is retrofitted, then the unstrengthened stem can easily control the failure of the section, often via concealed damage to internal strands. Corrosion damage in one stem is a strong indication of similar damage in the other. Therefore, it is safe to assume that each stem in a channel will exhibit a similar level of degradation whether said degradation is visible or not, and thus, both stems should thus be strengthened. The approach of always strengthening both stems in a prestressed channel beam also helps to ensure the flexural stiffness is balanced about the width of the cross-section, allowing both stems to deform evenly under load. Asymmetric stiffness, such as that created in WCS1 and WCS2 by strengthening only one stem, resulted in a component of torsion under load. This torsion effect was particularly evident in the test of WCS1 as the section twisted while deflecting vertically, amplifying stress in the concrete. Finally, strengthening both stems in a channel beam provides some added protection against the progression of degradation in the concrete and internal steel reinforcement that is likely to continue while a temporary MF-FRP repair remains in service.

6.2 Recommendations for the Service Life of the MF-FRP Retrofit System

Based on the results and analyses presented in Chapters 4 and 5, respectively, the lifespan of the MF-FRP retrofit system applied to degraded prestressed concrete channel beams can be reasonably taken as up to five years based on the fatigue tests conducted. Five years does slightly exceed the average conditions of the fatigue testing program (SCS3 reached 4.5 years and WCS3 reached 5.0 years of combined field and laboratory service), but the fatigue tests performed were conservative in terms of assumed AADT (trucks comprised 10% of all traffic), loading assumptions (all trucks assumed fully loaded), and testing of a single girder in isolation (no transverse load distribution). Furthermore, WCS3 demonstrated a remaining static capacity of 23.4 kips post-fatigue after 5 years of combined field and lab service, which is far above the 16 kip threshold. While SCS3 did not perform as well as WCS3, it still survived 4.5 years of combined field and lab loading before its capacity fell below the 16-kip threshold. Notably, the failure of SCS3 did not involve the MF-FRP system and was marked by an incremental loss of stiffness over time with significant visual indication of the accumulating degradation. Unstrengthened beams taken from the same bridges that did not have significant visual damage survived fewer years of equivalent service than the strengthened beams with heavy damage described above. The unstrengthened beams also degraded more rapidly at the end of service and had similar residual static capacities as compared with retrofitted beams. Notably, a 54-year-old beam strengthened in the laboratory with MF-FRP (no field service on the repair) survived 3.1 years of simulated field service on the repair with no apparent loss of stiffness, no visual degradation, and 37 kips of residual static capacity.

An important point regarding the lifespan of the MF-FRP system is that even after a five-year service life, the capacity of the MF-FRP repair was not limited by the FRP strap or the mechanical components of the MF-FRP system. Rather, long term capacity of prestressed channel members retrofitted with MF-FRP was limited by degradation mechanisms in the underlying concrete, such as crushing, splitting, spalling, and cracking. All of these degradation behaviors developed over time in the experimental program and were readily identified by visual inspection. It is noted that the recommended useful lifespan of an MF-FRP system is dependent on the AADT and original HS-15 inventory and operating loading conditions assumed in this research, but these assumptions will be conservative for many, although not all, channel beam bridges in North Carolina.

The ability of the MF-FRP system to restore the capacity of deficient beams was also clearly demonstrated by the static testing program conducted on beams with field-applied MF-FRP subjected to two years of field service post-repair. Strengthened specimens tested directly failure exhibited about 30 kips of residual capacity compared with about 23 kips in similar unstrengthened and visually undamaged specimens from the same bridges.

In summary, the 2-year service life recommended as a starting point in prior research for the MF-FRP system is overly conservative. The recommendation of the current research is to extend the maximum allowable service life of the MF-FRP system to 5 years, assuming regular visual inspections of the repaired beams. Inspections would ideally be conducted annually, especially as a beam reaches the end of its service life, as degradation can develop over a period of 6 months, as was the case for specimen SCS3. Regardless of the inspection interval chosen, the condition of a retrofitted beam should be documented well at the time of repair and should be monitored for changes over the service life of that repair.

7 Implementation and Technology Transfer Plan

It is envisioned that the MF-FRP repair will continue to be implemented on NCDOT prestressed concrete channel beam and cored slab bridges by the NCDOT Structures Management Unit (SMU) and NCDOT Division of Bridge Maintenance Offices. The MF-FRP system has been implemented by the SMU in a standard design and management sheet, which can simply be updated to include the recommendation of a maximum 5-year service life. Continued implementation of this retrofit system and a longer potential service life of the temporary MF-FRP repair will extend the service lives of existing bridges, allowing for more time between the identification of bridge replacement needs and completion of the actual bridge replacements. By extending the service life of the temporary retrofit system, this research allows the NCDOT greater flexibility in allocating resources across the State. In addition to implementation with the NCDOT, the findings of this research will be published in conference and journal papers, and discussions are underway with DOTs in other states to explore the use of the MF-FRP repair in their jurisdictions.

8 Conclusions

This report presents a research effort undertaken to address and fill knowledge gaps on the MF-FRP retrofit system that was previously developed and studied by (McCoy, 2019), (Bourara, 2019), and (Lin, 2021). The experimental testing program added 12 more specimens to the existing database of information on the system, consisting of static tests and novel fatigue tests on prestressed channel beams with and without the retrofit installed. Importantly, tests were conducted on beams repaired and then aged in the field, marking the first time the MF-FRP retrofit was studied after use in field service. This research contributed to the understanding of the MF-FRP retrofit system subjected to fatigue loading. It was found that the useful fatigue life of the MF-FRP system was significantly longer than that of the typical underlying prestressed concrete sections. In addition, continued field implementation of the system is underway, proving the effectiveness of the system at efficiently maintaining critical highway infrastructure.

The primary findings of this research are summarized as follows:

1. The MF-FRP retrofit system was proven to address both the inventory and operating load ratings through laboratory experiments. Static tests demonstrated the MF-FRP system was very effective at increasing load ratings when applied to both stems of a C-channel beam.

2. Prior to this work, available literature on prestressed concrete beams strengthened with the MF-FRP retrofit system did not contain any full-scale fatigue tests. This research adds additional static tests to the known database of experiments and, most importantly, adds the first full-scale fatigue tests, the results of which help quantify the service life of the retrofit system.

3. Results of experimental tests performed on C-channel specimens with the retrofit applied to only one stem proved unsatisfactory, with the load carrying capacity not meeting requirements due to deficient unstrengthened stems controlling performance. In addition, the observed failure modes in the unstrengthened stems were relatively brittle and sudden. Therefore, this work strongly recommends that the MF-FRP retrofit be applied to both stems of a C-channel beam to avoid these potential issues, regardless of the relative condition of the individual stems. If damage sufficient to warrant retrofit is observed in one stem, the other stem should be assumed damaged as well.

4. The full-scale fatigue tests demonstrated that fatigue damage in strengthened beams developed primarily in the concrete section and internal prestressing strands. The MF-FRP retrofit system remained tensioned and incurred no significant damage, even after years of combined field and simulated laboratory service. Based on this information, the original prestressed concrete beam will likely degrade under cyclic loading at a faster rate than will the MF-FRP retrofit system. As such, the condition of the original member must be thoroughly assessed before installation of the retrofit and the condition of the member and the MF-FRP system should be routinely monitored over the temporary life of the retrofit to prevent possible fatigue failures, which for the 54-year-old beams tested, are less likely to develop in damaged beams retrofit with MF-FRP than in similar undamaged beams subjected to the same loading.

5. The fatigue testing results demonstrated that channel members with two strengthened stems were able to resist fatigue cycles equivalent to up to 5 years of service. It is recommended that the service life of the MF-FRP system be increased to five years, provided that regular inspections and assessments take place, as degradation due to fatigue cycles was primarily confined within the original concrete section and internal steel reinforcement.

6. Although section shear capacity was not directly tested, the specimen that included the shear-strengthening plates (SCS1) performed well and failed in flexure, with no issues arising in the heavily deteriorated and repaired end regions.

7. The concrete compressive strength of each specimen was determined through the testing of cores. The concrete compressive strength measured from the cores demonstrated variability that did not correlate with damage level or flexural performance, indicating that concrete compressive strength alone is not a predictor of beam condition or level of corrosion.

8. Continued field implementation of the MF-FRP retrofit system demonstrates the effectiveness of the system and will likely expand within North Carolina and beyond.

REFERENCES

AASHTO. (2016). *The Manual for Bridge Evaluation, 2nd Ed.* Washington, D.C.: American Association of State Highway and Transportation Officials.

AASHTO. (2017). *LRFD Bridge Design Specifications, 8th Ed.* Washington, D.C.: American Association of State Highway and Transportation Officials.

AASHTO. (2018). *The Manual for Bridge Evaluation, 3rd Ed.* Washington, D.C.: American Association of State Highway and Transportation Officials.

ACI 214.4R. (2010). *Guide for Obtaining Cores and interpreting Compressive Strength Results.* Farmington Hills: ACI.

ASTM C39-24. (2024). *Standard Test method for Compressive Strength of Cylindrical Concrete Specimens.* West Conshohocken, PA: ASTM International.

ASTM C42-20. (2020). *Standard testing Method for Obtaining and Testing Drilled Cores and Sawed Beams of Concrete.* West Conshohocken, PA: ASTM International.

Bourara, Z. (2019). Long-Term Behavior and Modeling of Prestressed Mechanically-Fastened Fiber Reinforced Polymer Retrofit for Prestressed Concrete Bridge Elements. *(Master's dissertation)*. North Carolina State University.

Gann, J. K. (2025). *Behavior of FRP Repaired Prestressed Concrete Bridge Beams after Two Years in Service.* Raleigh: North Carolina State University.

Lin, S.-H. (2021). Analysis and Design of Deteriorated Prestressed Concrete Bridge Beams in Flexure and Shear Repaired with Prestressed Mechanically-Fastened Fiber-Reinforced Polymer. *(Doctoral dissertation)*. North Carolina State University.

McCoy, B. C. (2019). Design and Implementation of a New Retrofit for Prestressed Concrete Bridge Elements Using Mechanically Fastened Fiber-Reinforced Polymer. *(Doctoral dissertation)*. North Carolina State University.

NCDOT. (2023, 08). *FRP Repair System.* Raleigh, NC: North Carolina DOT.

NCDOT. (2024, September 30). *Traffic Volume Maps*. Retrieved from Connect NCDOT: https://connect.ncdot.gov/resources/State-Mapping/Pages/Traffic-Volume-Maps.aspx

NCDOT. (2025, January). *North Carolina Bridge Management System*. Retrieved September 22, 2023, from North Carolina Department of Transportation: https://www.ncdot.gov/initiatives-policies/Transportation/bridges/Pages/default.aspx

North Carolina DOT. (1966). *Standard prestressed concrete channels 20 ft.-, 25ft.-, and 30ft.- Spans, 24ft.- , 29ft.-, and 34ft.- roadways.* Raleigh, NC: North Carolina DOT.

APPENDIX A: Material for Bridge No. 070018 Retrofit

Table A-1 shows the required material needed to retrofit one entire C-channel beam for Bridge No. 070018. Figure A-1 shows the NCDOT FRP system repair document.

Table A-1: Parts needed for Bridge No. 070018 retrofit

Item	Quantity Needed for 2 stems	Note
½ in.-13 Bolts (1.5" Long) (Grade A325 Steel)	88	-
½ -13 in. Nuts (Steel – Grade 8)	88	-
½ in. Flat Washers	176	-
¾ in.-10 Bolts (8" Long) (Grade A325 Steel)	12	for stem with shear strengthening plate
¾ in.-10 Bolts (7" Long) (Grade A325 Steel)	12	for stem without shear strengthening plate
¾ -10 in. Nuts (Black-Oxide Steel – Grade 8)	24	-
¾ in. Flat Washers	24	-
0.812 in. Wedge Washers	24	-
5/8 in. -11 bolts (6" long) (Grade A325 Steel)	12	Bolts for shear strengthening plates
5/8 -11 in. Nuts (Black-Oxide Steel – Grade 8)	12	Nuts for shear strengthening plates
5/8 in. Flat Washers	12	Flat washers for shear strengthening plates
0.688 in. Wedge washers	12	Wedge washers for shear strengthening plates
FRP Plate	60 feet	
Shear strengthening plates	2	

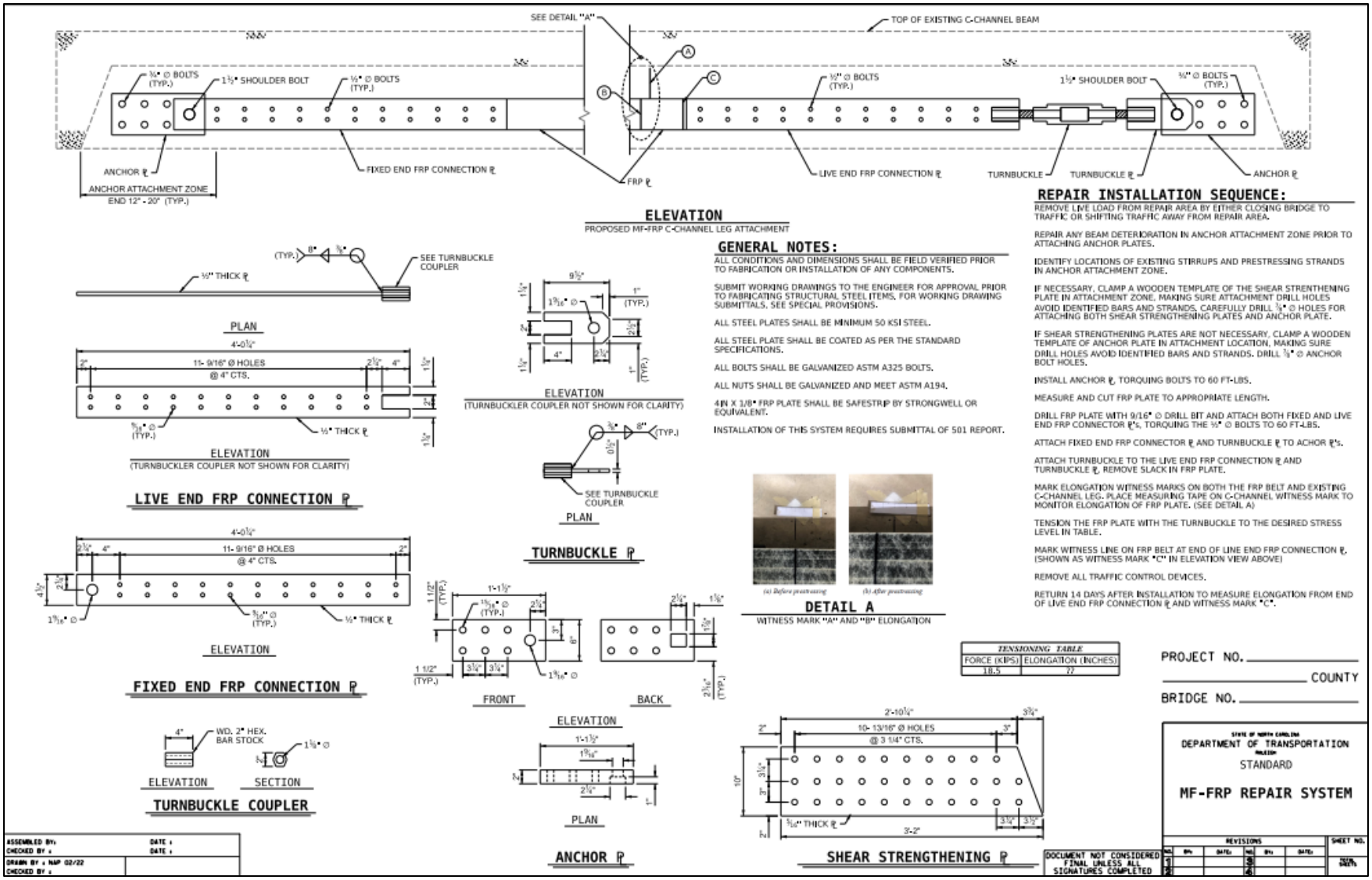

Figure A-1: NCDOT FRP Repair System Document (adapted from (NCDOT, 2023))